UNIVERSITY OF HELSINKI

https://helda.helsinki.fi

Selective synthesis of novel quinolones-amino esters as potential antibacterial and antifungal agents : Experimental, mechanistic study, docking and molecular dynamic simulations

Moussaoui, Oussama; Byadi, Said; Hachim, Mouhi Eddine; Sghyar, Riham; Bahsis, Lahoucine ...

2021-10-05
Elsevier B.V.
http://hdl.handle.net/10138/357737
Moussaoui, O, Byadi, S, Hachim, M E, Sghyar, R, Bahsis, L, Moslova, K, Aboulmouhajir, A, Rodi, Y K, Podlipnik, C, El Hadrami, E M & Chakroune, S 2021, 'Selective synthesis of novel quinolones-amino esters as potential antibacterial and antifungal agents : Experimental, mechanistic study, docking and molecular dynamic simulations', Journal of Molecular Structure, vol. 1241, 130652. https://doi.org/10.1016/j.molstruc.2021.130652

Downloaded from Helda, University of Helsinki institutional repository. https://helda.helsinki.fi
This is an electronic reprint of the original article.
This reprint may differ from the original in pagination and typographic detail.
Please cite the original version.

Selective synthesis of novel quinolones-amino esters as potential antibacterial and antifungal agents: Experimental, Mechanistic study, Docking and Molecular Dynamic Simulations

Oussama Moussaoui[a,*], Said Byadi[b], Mouhi Eddine Hachim[c], Riham Sghyar[a], Lahoucine Bahsis[c, d,*], Karina Moslova[e], Aziz Aboulmouhajir [b, f], Youssef Kandri Rodi[a], Črtomir Podlipnikf[g], El Mestafa EL Hadrami[a] and Said Chakroune[a]

[a] *Laboratory of Applied Organic Chemistry, Faculty of Science and Techniques, Sidi Mohamed Ben Abdellah University, B.P. 2202, Route d'Imouzzer, Fez, 30050, Morocco.*

[b] *Extraction, Spectroscopy and Valorization Team, Organic synthesis, Extraction and Valorization Laboratory, Faculty of Sciences of Ain Chock, Hassan II University, Casablanca, Morocco.*

[c] *Laboratoire de Chimie Analytique et Moléculaire, LCAM, Faculté Polydisciplinaire de Safi, Université Cadi Ayyad, 4162 Safi, Morocco.*

[d] *Laboratoire de Chimie de Coordination et d'Analytique, Département de Chimie, Faculté des Sciences d'El Jadida, Université Chouaïb Doukkali, El Jadida, Morocco.*

[e] *Department of Chemistry, University of Helsinki, FI-00014, Helsinki, Finland.*

[f] *Modeling and Molecular Spectroscopy Team, Faculty of Sciences, University Chouaib Doukkali, El-Jadida, Morocco.*

[g] *Faculty of Chemistry and Chemical Technology, University of Ljubljana, Večna pot 113, Ljubljana, Slovenia.*

Corresponding authors- Phone: +21254496534 (OM)

E-mails: oussama.moussaoui1208@gmail.com (OM); bahsis.l@ucd.ac.ma (LB).

Abstract:

A new selective synthesis of novel quinoline carboxamides was developed by the N-alkylation reaction of methyl (2-oxo-1,2- dihydroquinolin-4-yl)-L-alaninate via phase transfer catalysis in a basic medium at room temperature. The compounds were obtained in excellent yields (70-90%) and characterized by ^{1}H, ^{13}CNMR spectroscopy and mass spectra. In addition, theoretical

studies at B3LYP/6-311G(d,p) level were carried out to explain the observed selectivity of the N-alkylation reaction of compound **2**. The biological activities of the synthesized compounds were studied using some bacterial and fungal strains. The results show that compounds **3h** and **3i** exhibit stronger antibacterial activity against *Bacillus subtilis* and *Staphyloccocus aureus*. Compound **3e** showed high antifungal activity against *Candida Albicans* compared to other substituted quinoline carboxamides. Molecular docking and molecular dynamics studies were also carried out to investigate the binding affinities of some compounds with the target proteins, and the results were in good correlation with the experimental findings.

Keywords: Quinoline-carboxamide, N-alkylation, antibacterial activity, DFT study, Molecular Dynamics.

Highlights

1- Synthesis and design of new heterocyclic compounds based on quinolones-L-alaninate.

2- The chemical structure of the prepared compounds was confirmed by NMR spectroscopy and mass spectra analysis.

3- Antimicrobial and antifungal activities of the quinolone amino derivatives were studied.

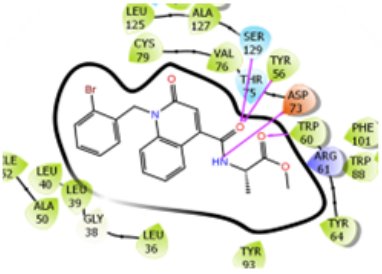
4- Quantum chemical calculations explained the observed selectivity of the N-alkylation reaction.

5- Docking and Molecular Dynamic simulations were used to explain the experimental biological activity results.

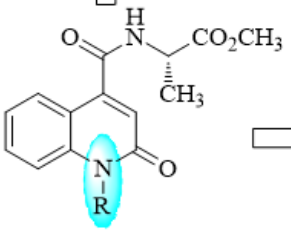
TOC

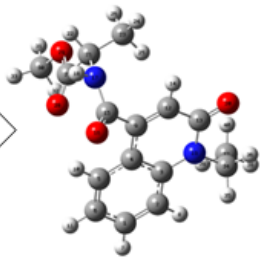


Antibacterial & Antifungal activities

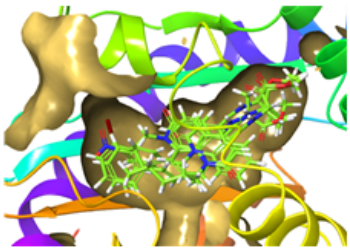


Docking Study





Mechanistic study



Molecular dynamic simulations

1. Introduction

Bacterial infections are responsible for millions of deaths each year due to ineffective antibacterial therapy. This situation is complicated by bacterial resistance to conventional antibiotics [1]. In 2017, the World Health Organisation (WHO) had announced the priority list of bacteria for which new antibiotics are urgently needed and for which *Pseudomonas aeruginosa* is a high priority [2]. They proliferate in the host body and activate the formation of a biofilm above a particular concentration of bacteria via the Quorum Detection System (QS) [3,4]. Bacterial biofilms are responsible for transmitting molecular signals involved in cellular communication to jointly decide how to adapt to the environment and activate defence mechanisms. Biofilms also support the expression of virulence genes, especially those responsible for drug resistance and antibiotics. They also form a physical barrier that blocks the penetration of substances such as antibiotics [5,6].

N-containing molecules, whether synthetic or natural, are essential and play a critical role in limiting bacterial resistance. Quinolines have received much attention because their intriguing physical and biological properties make them promising drug core structures [7-33]. In particular, the chemistry of 2-quinolone derivatives has received more attention in organic and medicinal chemistry. Several advances in the application of this family of compounds have been of great benefit. They are among the most synthesized antibiotics, which have been widely used to develop new antibacterial agents [34,35]. In this context, the development of new synthetic N-alkyl-2-quinolones represents an effective strategy and challenge for their synthesis and discovering new promising pharmacophore candidates that exhibit potent antibacterial activity. For example, Kumar and al. screened a new series of N-(3-acetyl-2-oxoquinolin-1(2H)-yl)benzamide (Figure 1a) for in vitro antimicrobial activity against *B. subtilis, S. aureus, E. coli,* and *P. aeruginosa,* comparable to ciprofloxacin as standard, and reported that some compounds showed potent antibacterial activity against gram-positive bacteria with MIC in the

range of 1.6-6.25 µg/mL [36]. Other compounds showed significant antibacterial activity against gram-negative bacteria with MIC ranging from 0.8 to 6.25 µg/mL.

Similarly, the synthesis of a series of s-triazine analogues was described by Patel and et *al*. (Figure 1b). They were biologically tested in vitro against two gram-positive bacteria (*S. aureus*, *B. cereus*) and six gram-negative bacteria (*E. coli*, *P. aeruginosa*, *K. pneumonia*, *S. typhi*, *P. vulgaris* and *S. flexneri*). The MIC values ranged from 6.25-25 µg/mL, and the compounds with quinolone moiety showed potential antimicrobial activity against *S. typhi* with MIC=12.5 µg/mL. Recently, Xue and *al*. reported the in vitro and in vivo antibacterial evaluation of a series of N-thiadiazole-4-hydroxy-2-quinolone-3-carboxamides (Figure 1c) against S. aureus and identified ten derivatives with better antibacterial activities with MIC below 1 µg/mL [38].

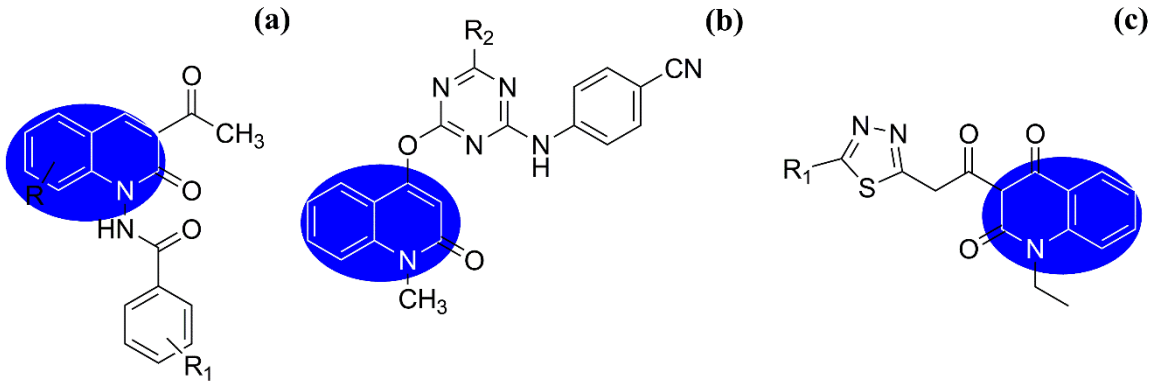


Figure 1. Some structures of 2-quinolone derivatives

Otherwise, as a non-natural amino acid, L-alanine derivatives are essential compounds for the synthesis of various biologically active molecules, such as the anti-Parkinsonian drug L-Dopa, [39], chemosensors [40], tricycles [41], chiral catalysts [42], aminoacyl tRNAs [43], benzo[a]quinolizidines [44] and anticancer agents [45]. In particular, quinoline synthesis from aniline is an excellent way for the production of various quinoline derivates. [46].

Our philosophy in this work was to synthesize novel hybrid molecules based on 2-quinolones derivatives and L-alanine-OMe (Figure 2) by N-alkylation of quinoline-carboxamide alaninate with nine alkylating agents. This combination aims to create new organic compounds that have become excellent active compounds with a broad spectrum of biological and pharmacological activities. We were able to synthesize 2-quinolone derivatives with broad-spectrum antibacterial and antifungal activities.

Molecular docking and molecular dynamics simulations (MD) were used to investigate the binding interactions of the compounds to the selected putative bacterial targets, in this study we interested in the Quorum Sensing (QS) target. The simulation results confirmed that these 2-quinolone derivatives could serve as potential antibacterial agents.

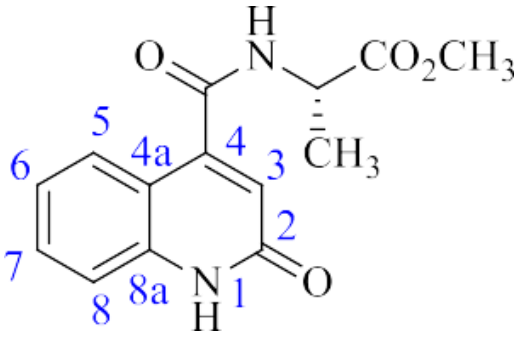


Figure 2. Structure of methyl (2-oxo-1,2-dihydroquinoline-4-yl)-L-alaninate

2. Materials and Methods

2.1. General Methods

The various reagents such as Alkyl bromide 98%, hexafluorophosphate benzotriazoletetramethyluronium (HBTU) 98%, triethylamine 99.5%, L- alanine 99%, tetrabutylammonium bromide (TBAB) 99%, potassium carbonate (K_2CO_3) 99%, anhydrous dimethylformamide 99.8%, ethyl acetate (HPLC-grade) and hexane (HPLC-grade) were purchased from Sigma-Aldrich.

Column liquid chromatography was performed on Merck silica gel 60 (230-400 mesh ASTM). Merck aluminium plates coated with Merck silica gel 60 F254 (0.2 mm thick) were used for thin-layer chromatography (TLC). The revelation of synthesized compounds was carried out by an ultraviolet lamp (UV) set at 254 nm. Their melting point was determined by a digital Electrothermal IA series 9000 fusiometer using capillary tubes.

NMR analyses were recorded using ~~on~~ the Bruker Ascend 400 MHz-Advance III HD NMR spectrometer (Bruker Corporation, Billerica, MA, USA). Besides, ^{1}H NMR spectra were recorded at 400 MHz, and ^{13}C NMR spectra at 100 MHz using DMSO-d_6 or $CDCl_3$ as solvent. The chemical shift (δ) of the different peaks was expressed in ppm and the coupling constants (nJ) in Hz. The following abbreviations were used to describe the variety of signals: Singlet (s), doublet (d), doublet doublet (dd), doublet doublet doublet (ddd), multiplet (m), triplet (t), and quadruplet (q).

The high-resolution mass spectra (ESI-TOF-MS) were measured ~~by~~ with the microTOF-MS instrument (Bruker Daltonics GmbH, Bremen, Germany) in positive electrospray ionization mode. During the pre-measurement, the instrument was calibrated with the 5 mM sodium formate solution.

2.2. Procedure for the preparation of methyl (2-oxo-1,2-dihydroquinoline-4-yl)-L-alaninate 2

A mixture of hexafluorophosphate benzotriazoletetramethyluronium (HBTU) (1.1 mol) and 2-oxo-1,2-dihydroquinoline-4-carboxylic acid (1 mol) in DMF (20 mL) was stirred for 10 min at room temperature. Then, 1.5 mol of protected amino acid solubilized was poured into the prepared mixture followed by the addition of 3.3 mol of triethylamine (TEA) in small amounts for 20 min at 0 °C. Further, the reaction was stirred at room temperature for 12 hours.

2.3. Procedure for the preparation of methyl 2-(3-oxo-4-(prop-2-yn-1-yl)-3,4-dihydro quinoline-1-carboxamid)propanoate 3a-3i

Methyl (2-oxo-1.2-dihydroquinolin-4-yl)-L-alaninate 2 (1.5 mol) and potassium carbonate K_2CO_3 (3 mol) were dissolved in dimethylformamide (25 mL). The solution was stirred for 5 minutes, then 0.01 equivalent of tetrabutylammonium bromide (TBAB) and 3 mol of alkylating agents were added. The mixture is stirred for 6 hours at room temperature. After reaction compilation, the organic phase was evaporated under reduced pressure. The residue obtained was ~~is~~ dissolved in dichloromethane and washed with water. The organic phase was ~~is~~ dried using ~~on~~ Na_2SO_4 and then concentrated under a vacuum. The product obtained was ~~is~~ purified by chromatography on a silica gel column.

2.3. Characterization:

2.3.1. Methyl 2-(1-ethyl-2-oxo-1,2-dihydroquinoline-4-carboxamido)propanoate: ***3a***

Yield: 90%, white solid, mp= 110-112 °C, Rf= 0.3 (hexane/ ethyl acetate: 1/1). NMR ^{1}H δ (ppm) 400 MHz, $CDCl_3$: 7.99 (dd, 1H, $^3J_{H-H}$= 8.1 Hz, $^4J_{H-H}$=1.5Hz, H_{ar}), 7.61 (ddd, 1H, $^3J_{H-H}$= 8.7 HZ, $^3J_{H-H}$= 7.2 HZ, ^{4}J=1.5 Hz, H_{ar}), 7.37 -7.26 (m, 2H, H_{ar}), 7.12 (d, 1H, $^3J_{H-H}$=7.4 Hz, NH), 6.83 (s, 1H, $CH_{ethylenic}$), 4.84 (qd, 1H, $^3J_{H-H}$=7.4 Hz, $^3J_{H-H}$=7.2 Hz, *CH-N), 4.28 (dt, 1H, $^2J_{H-H}$=14.1 Hz, $^3J_{H-H}$=7.1 Hz, CH_2-N), 4.15 (dt, 1H, $^2J_{H-H}$=14.1 Hz, $^3J_{H-H}$=7.1 Hz, CH_2-N), 3.84 (s, 3H, CH_3-O), 1.64 (d, 3H, $^3J_{H-H}$=7.2 Hz, CH_3), 1.28 (d, 3H, $^3J_{H-H}$=7.1Hz, CH_3). NMR ^{13}C δ (ppm) 100 MHz, $CDCl_3$: 172.85 ($C{=}O_{ester}$), 165.06 ($C{=}O_{amide}$), 161.00 ($C{=}O_{amide\ quinoline}$), 144.73-139.14 (C_{4a}-C_{8a}), 131.14 (Ct_5), 127.44 (Ct_7), 122.60 ($=Ct_{ethylenic}$), 119.66 (Ct_6), 117.78 ($Cq_{ethylenic}$), 114.34 (Ct_8), 52.72 (*CH-N), 48.54 (CH_3-O), 37.38 (N-CH_2), 18.08 (CH_3), 12.59 (CH_3-CH_2). Mass spectrometry (ESI-TOFMS): *m/z* calculated for $[C_{16}H_{18}N_2O_4+Na]^+$ 325.1159, found 325.1153; *m/z* calculated for $[(C_{16}H_{18}N_2O_4)_2+Na]^+$ 627.2425, found 627.2486.

2.3.2. Methyl 2-(2-oxo-1-pentyl-1,2-dihydroquinoline-4-carboxamido)propanoate: ***3b***

Yield: 87%, white solid, mp= 134-136 °C, Rf= 0.35 (hexane/ ethyl acetate: 1/1). NMR ^{1}H δ (ppm) 400 MHz, $CDCl_3$: 7.98 (dd, 1H, $^{3}J_{H-H}$= 8.1 Hz, $^{4}J_{H-H}$=1.5Hz, H_{ar}), 7.61 (ddd, 1H, $^{3}J_{H-H}$= 8.7 HZ, $^{3}J_{H-H}$= 7.2 HZ, $^{4}J_{H-H}$=1.5 Hz, H_{ar}), 7.37 -7.26 (m, 2H, H_{ar}), 6.83 (s, 1H, $CH_{ethylenic}$), 6.78 (d, 1H, $^{3}J_{H-H}$=7.4 Hz, NH), 4.85 (qd, 1H, $^{3}J_{H-H}$=7.4 Hz, $^{3}J_{H-H}$=7.2 Hz, *CH-N), 4.26 (m, 2H, CH_2-N), 3.85 (s, 3H, CH3-O), 1.72(m, 2H, CH_2), 1.59 (d, 3H, $^{3}J_{H-H}$=7.2 Hz, CH_3), 1.51- 1.34 (m, 4H, CH_2), 1.28 (d, 3H, $^{3}J_{H-H}$=7 Hz, CH_3-CH_2). NMR ^{13}C δ (ppm) 100 MHz, $CDCl_3$: 172.81 ($C=O_{ester}$), 165.98 ($C=O_{amide}$), 161.15 ($C=O_{amide\ quinoline}$), 144.47-139.55 (C_{4a}-C_{8a}), 131.36 (Ct_5), 127.31 (Ct_7), 122.51 ($=Ct_{ethylenic}$), 119.80 (Ct_6), 117.66 ($Cq_{ethylenic}$), 114.55 (Ct_8), 52.76 (*CH-N), 48.52 (CH_3-O), 42.36 (N-CH_2), 29.09 (CH_2), 27.14 (CH_2), 23.45 (CH_2), 18.08 (CH_3), 14.01 (CH_3-CH_2). Mass spectrometry (ESI-TOFMS): *m/z* calculated for $[C_{19}H_{24}N_2O_4+Na]^+$ 367.1628, found 367.1621; *m/z* calculated for $[(C_{19}H_{24}N_2O_4)_2+Na]^+$ 711.3364, found 711.3365.

2.3.3. Methyl 2-(1-hexyl-2-oxo-1,2-dihydroquinoline-4-carboxamido)propanoate: ***3c***

Yield: 85%, white solid, mp= 120-122 °C, Rf= 0.4 (hexane/ ethyl acetate: 1/1). NMR ^{1}H δ (ppm) 400 MHz, $CDCl_3$: 7.99 (dd, 1H, $^{3}J_{H-H}$= 8.1 Hz, $^{3}J_{H-H}$ =1.5Hz, Har), 7.61(ddd, 1H, $^{3}J_{H-H}$= 8.7 HZ, $^{3}J_{H-H}$= 7.2 HZ, $^{4}J_{H-H}$=1.5 Hz, H_{ar}), 7.37 -7.26 (m, 2H, H_{ar}), 6.82 (s, 1H, $CH_{ethylenic}$), 6.67 (d, 1H, $^{3}J_{H-H}$=7.4Hz, NH), 4.85 (qd, 1H, $^{3}J_{H-H}$=7.4 Hz, $^{3}J_{H-H}$=7.2 Hz, *CH-N), 4.30(m, 1H, CH_2-N), 3.87 (m, 1H, CH_2-N) 3.85 (s, 3H, CH_3-O), 1.76 (m, 2H, CH_2), 1.59 (d, 3H, $^{3}J_{H-H}$=7.2 Hz, CH_3), 1.57-1.18 (m, 9H, CH_2 et CH_3). NMR ^{13}C δ (ppm) 100 MHz, $CDCl_3$: 172.66 ($C=O_{ester}$), 165.88 ($C=O_{amide}$), 161.08 ($C=O_{amide\ quinoline}$), 144.45-139.76 (C_{4a}-C_{8a}), 131.37 (Ct_5), 127.29 (Ct_7), 122.52 ($=Ct_{ethylenic}$), 119.80 (Ct_6), 117. 72 ($Cq_{ethylenic}$), 114.56 (Ct_8), 52.76 (*CH-N), 48.52 (CH_3-O), 42.56 (N-CH_2), 30.79 (CH_2), 27.42 (CH_2), 26.94 (CH_2), 22.60 (CH_2), 18.23 (CH_3), 14.03 (CH_3-CH_2). Mass spectrometry (ESI-TOFMS): *m/z* calculated for $[C_{20}H_{26}N_2O_4+H]^+$ 359.1965, found 359.1964; *m/z* calculated for $[C_{20}H_{26}N_2O_4+Na]^+$ 381.1785, found 381.1792; *m/z* calculated for $[(C_{20}H_{26}N_2O_4)_2+Na]^+$ 739.3677, found 739.3718.

2.3.4. Methyl 2-(1-allyl-2-oxo-1,2-dihydroquinoline-4-carboxamido)propanoate: **3d**

Yield: 80%, white solid, mp= 120-122 °C, Rf= 0.28 (hexane/ ethyl acetate: 1/1). NMR ^{1}H δ (ppm) 400 MHz, $CDCl_3$: 7.98 (dd, 1H, ^{3}J = 8.1 Hz, ^{4}J=1.5Hz, Har), 7.60 (ddd, 1H, ^{3}J = 8.7 HZ, ^{3}J = 7.2 HZ, ^{4}J=1.5 Hz, H_{ar}), 7.37 -7.26 (m, 2H, H_{ar}), 6.87 (s, 1H, $CH_{ethylenic}$), 6.79 (d, 1H, $^{3}J_{H-H}$=7.4 Hz, NH), 5.96 (m, 1H, CH-CH_2), 5.25 (dd, 1H, =CH_2), 5.13 (dd, 1H, =CH_2),4.97 (d, 2H, $^{3}J_{H-H}$= 7.2 HZ, CH_2-N), 4.85 (qd, 1H, $^{3}J_{H-H}$=7.4 Hz, $^{3}J_{H-H}$=7.2 Hz, *CH-N), 3.85 (s, 3H, CH_3-O), 1.59 (d, 3H, $^{3}J_{H-H}$=7.2 Hz, CH_3). NMR ^{13}C DEPT 135 δ (ppm) 100 MHz, $CDCl_3$: 131.40 (Ct_5), 131.28 (CH=CH_2), 127.15 (Ct_7), 122.78 (=$Ct_{ethylenic}$), 119.80 (Ct_6), 117. 6 (CH_2=CH), 115.23 (Ct_8), 52.78 (*CH-N), 48.54 (CH_3-O), 44.73 (N-CH_2), 18.23 (CH_3). Mass spectrometry (ESI-TOFMS): *m/z* calculated for $[C_{17}H_{18}N_2O_4+Na]^+$ 337.1159, found 337.1167, *m/z* calculated for $[(C_{17}H_{18}N_2O_4)2+Na]^+$ 651.2425, found 651.2471.

2.3.5. Methyl 2-(1-(2-ethoxy-2-oxoethyl)-2-oxo-1,2-dihydroquine-4-carboxamido)propanoate: **3e**

Yield: 83%, White solid, mp= 168-170 °C, Rf= 0.30 (hexane/ ethyl acetate: 1/1). NMR ^{1}H δ (ppm) 400 MHz, $CDCl_3$: 7.98 (dd, 1H, $^{3}J_{H-H}$ = 8 Hz, $^{4}J_{H-H}$= 1.4Hz, H_{ar}), 7.58 (td, 1H, $^{3}J_{H-H}$= 7.2 HZ, $^{4}J_{H-H}$=1.5 Hz, H_{ar}), 7.52 (dd, 1H, $^{3}J_{H-H}$= 8.1 HZ, $^{3}J_{H-H}$= 1.5 Hz, H_{ar}), 7.33-7.28 (m, 2H, H_{ar}), 7.12 (d, 1H, $^{3}J_{H-H}$= 7.2 Hz, NH), 6.82 (s, 1H, $CH_{ethylenic}$), 5.07-5.03 (m, 2H, CH_2-NH), 4.80 (qd, 1H, $^{3}J_{H-H}$=7.2 Hz, $^{3}J_{H-H}$= 7.2 Hz, *CH-N), 4.22(q, 2H, $^{3}J_{H-H}$= 6.7 Hz, CH_2-O), 3.84 (s, 3H, CH_3- O), 1.57 (d, 3H, $^{3}J_{H-H}$= 7.2 Hz, CH_3), 1.35 (t, 3H, $^{3}J_{H-H}$= 6.7 Hz, CH_3-CH_2). NMR ^{13}C δ (ppm) 100 MHz, $CDCl_3$: 172.27 (C=O_{ester}), 167.75 (C=O_{amide}), 165.85 (C=$O_{amide\ quinoline}$), 161.14 (C=O_{ester}), 145.50-139.55 (C_{4a}-C_{8a}), 131.63 (Ct_5), 127.51 (Ct_7), 123.08 (=$Ct_{ethylenic}$), 119.22 (Ct_6), 117.61($Cq_{ethylenic}$), 113.90 (Ct_8), 61.88 (N-CH_2), 52.68 (*CH-N), 48.55 (CH_3-O), 43.82(CH_2-O), 17.91 (CH_3), 14.10 (CH_3). Mass spectrometry (ESI-TOFMS): *m/z* calculated for

$[C_{18}H_{20}N_2O_6+Na]^+$ 383.1214, found 383.1218, *m/z* calculated for $[(C_{18}H_{20}N_2O_6)2+Na]^+$ 743.2535, found 743.2539 .

2.3.6. Methyl 2-(1-(2-methylbenzyl)-2-oxo-1,2-dihydroquinoline-4-carboxamido)propanoate: ***3f***

Yield: 79%, white solid, mp= 153-155 °C, Rf= 0.30 (hexane/ ethyl acetate: 1/1). NMR ^{1}H δ (ppm) 400 MHz, $CDCl_3$: 8.02 (dd, 1H, $^3J_{H-H}$= 8.1 Hz, $^2J_{H-H}$=1.5 Hz, H_{ar}), 7.46 (ddd, 1H, ^{3}J= 8.6 Hz, $^3J_{H-H}$= 7.1 Hz, $^2J_{H-H}$= 1.5 Hz, H_{ar}), 7.30-7.20 (m, 2H, H_{ar}), 7.16 (d, 1H, $^3J_{H-H}$= 7.5 Hz, H_{ar}), 7.07-6.97 (m, 2H, H_{ar}), 6.94 (s, 1H, $CH_{ethylenic}$), 6.56 (d, 1H, $^3J_{H-H}$= 7.7 Hz, NH) , 5.51-5.32 (m, 2H, CH_2-N), 4.82 (qd, 1H, ^{3}JH-H= 7.5 Hz, $^3J_{H-H}$= 7.2 Hz, *CH-N), 3.85 (s, 3H, CH_3-O), 1.67 (s, 3H, CH-Ar), 1.59 (d, 3H, $^3J_{H-H}$= 7.2 Hz, CH_3). NMR ^{13}C δ (ppm) 100 MHz, $CDCl_3$: 172.82 ($C{=}O_{ester}$), 166.84 ($C{=}O_{amide}$), 165.92 ($C{=}O_{amide\ quinoline}$), 145.18-139.79 (C_{4a}-C_{8a}), 134.83 (Ct_{ar}), 132.95 (Ct_{ar}), 131.57 (Ct_5), 130.47 (Ct_q), 127.22 (Ct_{ar}), 127.15 (Ct_7), 126.39 (Ct_{ar}),124.43 (Ct_{ar}), 122.94 ($=Ct_{ethylenic}$), 119.59 (Ct_6), 117.70 ($Cq_{ethylenic}$), 115.54 (Ct_8), 52.78 (*CH-N), 48.58 (CH_3-O), 44.17 (N-CH_2), 18.19 (CH_3), 14.12 (CH_3-Ar). Mass spectrometry (ESI-TOFMS): *m/z* calculated for $[C_{22}H_{22}N_2O_4+Na]^+$ 401.1472, found 401.1461, *m/z* calculated for $[(C_{22}H_{22}N_2O_4)2+Na]^+$ 779.3051, found 779.3099.

2.3.7. Methyl 2-(1-(4-nitrobenzyl)-2-oxo-1,2-dihydroquinoline-4-carboxamido)propanoate: ***3g***

Yield: 75%, White solid, mp= 218-220 °C, Rf= 0.30 (hexane/ ethyl acetate: 1/1). NMR ^{1}H δ (ppm) 400 MHz, $CDCl_3$: 8.18 (d, 2H, $^3J_{H-H}$ = 9.6 Hz, H_{ar}), 8.02 (dd, 1H, $^3J_{H-H}$= 8.1 Hz, $^2J_{H-H}$=1.5 Hz, H_{ar}), 7.51 (ddd, 1H, $^3J_{H-H}$=8.5 Hz, ^{3}J=7.1 Hz, $^2J_{H-H}$=1.5Hz, H_{ar}), 7.38 (d, 2H, $^3J_{H-H}$= 9.6 Hz, H_{ar}), 7.29 (m, 1H, H_{ar}), 7.16 (d, 1H, $^3J_{H-H}$=8.5 Hz, H_{ar}), 6.95 (s, 1H, $CH_{ethylenic}$), 6.75 (d, 1H, $^3J_{H-H}$= 7.5 Hz, NH) , 5.655 (m, 2H, CH_2-N), 4.87 (qd, 1H, $^3J_{H-H}$= 7.5 Hz, $^3J_{H-H}$= 7.2 Hz, *CH-N), 3.86 (s, 3H, CH_3-O), 1.62 (d, 3H, $^3J_{H-H}$=7.2 Hz, CH_3). NMR ^{13}C δ (ppm) 100 MHz,

$CDCl_3$: 172.80 ($C=O_{ester}$), 165.56 ($C=O_{amide}$), 165.43($C=O_{amide\ quinoline}$), 147.43 (Cq_{ar}), 145.53-139.79 (C_{4a}-C_{8a}), 143.37 (Ct_{ar}), 131.81 (Ct_5), 127.63 (Ct_7), 124.20 (Ct_{ar}), 123.32 ($=Ct_{ethylenic}$), 119.48 (Ct_6), 117.77($Cq_{ethylenic}$), 114.81 (Ct_8), 52.86 (*CH-N), 48.61 (CH_3-O), 45.62 (N-CH_2), 18.30 (CH_3). Mass spectrometry (ESI-TOFMS): *m/z* calculated for $[C_{21}H_{19}N_3O_6+Na]^+$ 432.1166, found 432.1162, *m/z* calculated for $[(C_{21}H_{19}N_3O_6)2+Na]^+$ 841.2440, found 841.2499.

2.3.8. Methyl 2-(1-(2-bromobenzyl)-2-oxo-1,2-dihydroquinoline-4-carboxamido)propanoate: ***3h***

Yield : 70%, white solid, mp= 172-174 °C, Rf= 0.30 (hexane/ ethyl acetate : 1/1). NMR ^1H δ (ppm) 400 MHz, $CDCl_3$: 8.01 (dd, 1H, $^3J_{H-H}$ = 8.1 Hz, $^2J_{H-H}$=1.5 Hz, Har), 7.64 (m, 1H, H_{ar}), 7.50 (ddd, 1H, $^3J_{H-H}$= 8.5 Hz, $^3J_{H-H}$= 7.1 Hz, $^2J_{H-H}$=1.5 Hz, H_{ar}), 7.28 (m, 1H, H_{ar}), 7.13 (m, 1H, H_{ar}), 7.05 (d, 1H, $^3J_{H-H}$=8.5 Hz, H_{ar}), 7.00 (d, 1H, $^3J_{H-H}$=7.4 Hz, NH) , 6.94 (s, 1H, $CH_{ethylenic}$), 6.67 (m, 1H, H_{ar}), 5.53 (m, 2H, CH_2-N), 4.87 (qd, 1H, $^3J_{H-H}$=7.4 Hz, $^3J_{H-H}$=7.2 Hz, *CH-N), 3.85 (s, 3H, CH_3-O), 1.61 (d, 3H, $^3J_{H-H}$=7.2 Hz, CH_3). NMR ^{13}C δ (ppm) 100 MHz, $CDCl_3$: 172.80 ($C=O_{ester}$), 165.56 ($C=O_{amide}$), 165.43($C=O_{amide\ quinoline}$), 147.43 (Cq_{ar}), 145.53-139.79 (C_{4a}-C_{8a}), 143.37 (Ct_{ar}), 131.81 (Ct_5), 127.63 (Ct_7), 124.20 (Ct_{ar}), 123.32 ($=Ct_{ethylenic}$), 119.48 (Ct_6), 117.77 ($Cq_{ethylenic}$), 114.81 (Ct_8), 52.86 (*CH-N), 48.61 (CH_3-O), 45.62 (N-CH_2), 18.30 (CH_3). Mass spectrometry (ESI-TOFMS): *m/z* calculated for $[C_{21}H_{19}N_2O_4+Na]^+$ 464.0356, found 464.0352, *m/z* calculated for $[(C_{21}H_{19}N_2O_4)_2+Na]^+$ 907.0332, found 907.0328.

2.3.9. Methyl 2-(2-oxo-1-(3-phenylallyl)-1,2-dihydroquinoline-4-carboxamido)propanoate: **3i**

Yield: 74%, white solid, mp= 140-142 °C, Rf= 0.30 (hexane / ethyl acetate: 1/1). NMR ^1H δ (ppm) 400 MHz, $CDCl_3$: 8.0 (dd, 1H, $^3J_{H-H}$= 8.1 Hz, $^2J_{H-H}$=1.5 Hz, H_{ar}), 7.59 (ddd, 1H, $^3J_{H-H}$=8.5 Hz, $^3J_{H-H}$=7.1 Hz, $^2J_{H-H}$=1.5 Hz, H_{ar}), 7.43 (m, 1H, H_{ar}), 7.30-7.18 (m, 6H, H_{ar}), 6.89 (s, 1H, $CH_{ethylenic}$), 6.83 (d, 1H, $^3J_{H-H}$= 7.3 Hz, NH) , 6.67 (m, 1H, H_{ar}), 6.52 (dt, 1H, , $^3J_{H-H}$= 16.1

Hz, $^{4}J_{H-H}$= 1.7 Hz, =CH-Ar), 5.29 (dt, 1H, $^{3}J_{H-H}$= 16.0 Hz, $^{3}J_{H-H}$= 5.4 Hz, =CH-CH_2), 5.12 (dd, 1H, $^{2}J_{H-H}$=18.0 Hz, $^{3}J_{H-H}$= 5.4 Hz, $^{4}J_{H-H}$= 1.7 Hz, CH_2-N), 5.06 (ddd, 1H, $^{2}J_{H-H}$= 18.0 Hz, $^{3}J_{H-H}$= 5.4 Hz, $^{4}J_{H-H}$= 1.7 Hz, CH_2-N), 4.86 (qd, 1H, $^{3}J_{H-H}$= 7.3 Hz, $^{3}J_{H-H}$=5.4 Hz, *CH-N), 3.85 (s, 3H, CH_3-O), 1.61 (d, 3H, $^{3}J_{H-H}$=7.2 Hz, CH_3). NMR ^{13}C δ (ppm) 100 MHz, $CDCl_3$: 172.82 ($C=O_{ester}$), 165.89 ($C=O_{amide}$), 161.14 ($C=O_{amide\ quinoline}$), 156.86 (Cq_{ar}), 144.95-139.70 (C_{4a}-C_{8a}), 136.15 (Cq_{ar}), 132.67 (Ct_5), 131.51 (=CH), 128.56 (Ct_{ar}), 127.87 (Ct_7), 127.24 (Ct_{ar}), 126.42 (Ct_{ar}), 122.83 ($=Ct_{ethylenic}$), 122.83 (=CH), 119.71 (Ct_6), 117.64($Cq_{ethylenic}$), 115.16 (Ct8), 52.79 (*CH-N), 48.56 (CH_3-O), 44.26 (N-CH_2), 18.24 (CH_3). Mass spectrometry (ESI-TOFMS): *m/z* calculated for $[C_{23}H_{22}N_2O_4+Na]^+$ 413.1472, found 413.1466, *m/z* calculated for $[(C_{23}H_{22}N_2O_4)_2+Na]^+$ 803.3051, found 803.3119.

2.4. Computational details

The quantum chemical calculations were performed with GAUSSIAN 09W program using B3LYP Density Functional Theory (DFT) functional using 6-311G(d,p) basis set [47,48].

All frequencies obtained were positive, which proves that the structure corresponds to minimum energy [49-51]. The electronic chemical potential (μ) and chemical hardness (η) were calculated using energies of the frontier molecular orbital HOMO (E_H) and LUMO (E_L) using the following expressions $\mu = (E_H + E_L)/2$ and $\eta = (E_L - E_H)$, respectively. The global electrophilicity (ω) and nucleophilicity (N) indexes were measured at the same level, and were given by the following simple expressions: $\omega = \mu^2 / 2\eta$; $N = E_H - E_H$ (tetracyanoethylene (TCE)) [52–54]. The Parr function was calculated with the help of the Mulliken atomic spin densities [55-57].

2.4. Biological assays

2.4.1. Disc Diffusion Method

The Agar Disc Diffusion (ADD) method was used to determine the tested products antibacterial activities. The test samples were dissolved in dimethyl sulfoxide (1%) (DMSO), which did not affect microbial growth. The test was performed in sterile Petri dishes containing agar medium. The sterilized medium (30 mL) was poured into clean Petri dishes. After solidification, 100 µL of fresh cultures of bacterial species (one microorganism per petri dish) were added. Similarly, sterile filter paper discs (6 mm in diameter) were impregnated with 6 µL of 10 mg/mL samples and then incubated at 37°C for 24 hours [58]. The inhibition zone diameter was measured in millimetres; an average of three independent determinations was taken.

2.4.2. Microdilution method

Minimum inhibitory concentration (MIC) values of the prepared compounds were determined using the Broth microdilution method [59]. A 96-well polypropylene microlitre plate was filled with 50 µL of Mueller- Hinton broth (MHB). Then, this step was followed by the addition of 50 µL of each sample at a final concentration of 10 mg/mL to the first well. Further dilutions of the ½ series were made by pipetting 50 µL from the first well and transferred to the next well. This step was repeated to the 12th well, and the final 50 µL mixture was discarded. As a final step, a 50 µL volume of bacterial solution was added to each well at a final concentration of approximately 106 CFU/mL. The 96 wells were then covered and incubated at 37°C for 24 hours, while the plates containing fungal organisms were incubated at 28°C for 48 hours. Subsequently, resazurin 5 µL was pipetted into all wells and incubated again at 37 °C for 2 hours. The MIC was reported as the lowest concentration that showed negative bacterial growth resulting in no change in the resazurin colour. A positive concentration is detected by reducing blue resazurin to pink resazurin [60]. The MIC determination was performed in triplicate for each organism, and the experiment was repeated if necessary.

2.5. Molecular docking and molecular dynamics

2.5.1. Choice of the bacterial target

Bacteria synthesize signaling macromolecules called autoinducers, which help them to communicate and evaluate their population. When the level of autoinducer is too low, bacteria proliferate to increase their number. When a threshold quantity is reached, the virulence increases, biofilm formation and auto-induction of their synthesis occur [61]. This type of behavior in bacteria is known as quorum sensing (QS). Therefore, quorum sensing (QS) is a potential target for new antimicrobial agents that prevent QS activation in vivo and reduce virulence. QS does not directly contribute to the growth of bacteria, so blocking effects of QS substances does not impose selective pressure for the emergence of resistance [62-64]. Theoretical analysis is used in this contribution to find the structural and chemical features of the investigated molecules, which may affect the QS circuit.

The *Pseudomonas aeruginosa* system has been one of the most intensively investigated quorum-sensing systems. Its importance is due to the potentially fatal effects of their infections, which kill many thousands of immune-compromised patients each year worldwide [65]. The opportunistic pathogen that causes death in most patients with cystic fibrosis, AIDS, and burns victims is *P. aeruginosa* [66]. For these reasons, as stated above, circuits of quorum sensing present in *Pseudomonas aeruginosa* are considered potential targets for developing potential compounds with anti-quorum sensing activity. Many studies and much research have been devoted to synthesizing and evaluating new candidates capable of modulating the quorum-sensing circuit present in *Pseudomonas aeruginosa* [67–69]. It is necessary to understand their inhibition mechanisms to find new candidate work for the QS circuit modulators. The structure of signaling molecules (AIs), analog structures of those AIs, and finally, the receptor proteins' structures help analyze the molecular interactions between ligands and the binding site.

2.5.2. Molecular docking

A theoretical analysis is used to find the structural and chemical features of this particular group of molecules that may affect the QS circuit. In the present study, we examined the poses of each inhibitor from Figure 3 within the binding site of the transcriptional receptor LasR using the docking program Glide implemented in Schrödinger Suite ver 18.1 [64]. The docking procedure began with the preparation of the receptor structure. The structure of LasR in complex with N-3-oxo-dodecanoyl-L-homoserine lactone was downloaded directly from Protein Data Bank (PDB code 3IX3) [70] into the Maestro GUI of Schrodinger Suite. The downloaded structure was then prepared for docking using the Protein Preparation Wizard utility of Schrodinger Suite, which summarizes, automates, and integrates the most commonly used tools and techniques in structure preparation. The prepared complex was used to create the interaction lattice necessary for Glide docking. The inhibitors' structures (Fig. 3.) were prepared using the LigPrep utility, and finally, Glide was used for molecular docking.

2.5.3. Molecular dynamics

MD simulation techniques were used to analyze the dynamic behaviour of the LasR protein's crystalline structures, which is a primary *P. aeruginosa* QS transcriptional activator and plays a pivotal role in the activation of many virulence genes. The LasR protein complex with the compound 3h used for MD simulation was obtained from a previous docking experiment.

MD simulation was conducted using the YASARA Dynamics software version 18.4.24.W.64 [71]. In MD simulations, the AMBER14 force field was used under periodic boundary conditions and explicit TIP3P water [72,73]. Multiple time steps of 1.25 fs for intramolecular and 2.5 fs for intermolecular forces were used. The initial configuration consisted of the protein-inhibitor complex in a cubic box with a length of 74.54 Å, and the remaining available space in the box was filled with TIP3P water molecules [73]. The final density of the water objects in the simulation box was 0.997 g cm^{-3}. A cut-off of 8.0 Å was used for the Lennard-Jones forces. The particle mesh Ewald method was used to treat the electrostatics. At the beginning of the calculations, the system's energy was minimized by simulated annealing; then, the dynamics

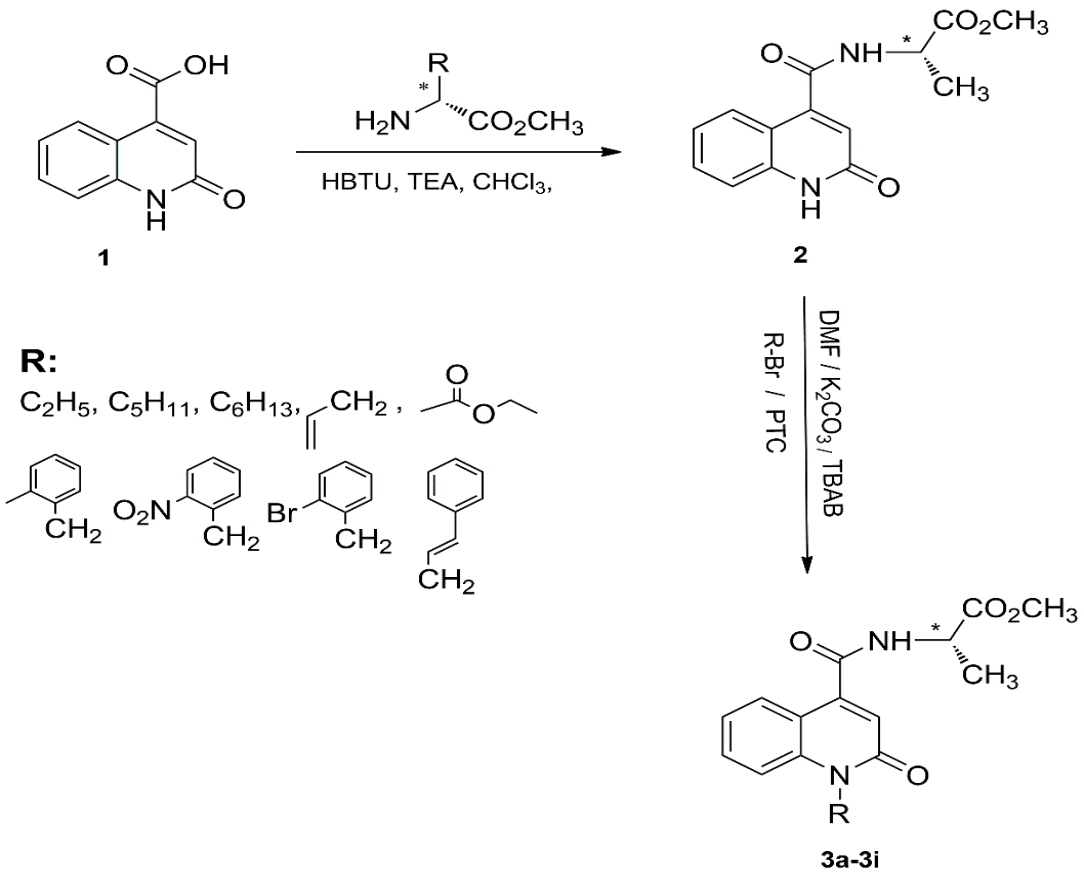
simulations were carried out at 298 K. The temperature was set using a Berendsen thermostat based on the time-averaged temperature.

The force field parameters for inhibitor 3h were determined using the YASARA-AutoSMILES multistep procedure. The procedure used SMILES strings to identify known molecules (even if residue and atom names differ) and resorts to the AM1BCC and general AMBER force field approaches for all other molecules [72, 74]. The AM1BCC charges were further improved by using known RESP (restrained electrostatic potential) charges of similar molecular fragments, which in turn were identified using SMILES strings [74]. A total of 250 ns MD were performed for the system, and snapshots were saved every 0.1 ns for further analysis [75]. In analyzing the MD trajectory, we focused on interpreting the following data: RMSD (Root Mean Square Deviation), RMSF (Root Mean Square Fluctuation), Rg (Radius of Gyration), SASA (Solvent Accessible Surface Area), the total number of hydrogen bonds and secondary structure fractions of the protein in the complex [76-78].

3. Results and discussion

3.1. Synthesis and characterization

First, the synthesis of quinoline carboxamide alaninate (2) was achieved by a coupling reaction between the 2-oxo-1,2-dihydroquinoline-4-carboxylic acid (1) and L-alanine-OMe in the presence of HBTU as an activating agent in a basic medium using triethylamine (TEA) in chloroform ($CHCl_3$) during 12 hours at room temperature (Scheme 1).



Scheme 1. Synthesis of N-alkylated quinolone-carboxamides (**3a-3i**)

The reaction of the 2-oxo-1,2-dihydroquinoline-4-carboxamides with different alkyl bromides under phase transfer catalysis (PTC) conditions [79], in dimethylformamide as a solvent in the presence of potassium carbonate and tetra butyl ammonium bromide (TBAB) leads to N-alkylated-carboxamides with good to excellent yields. The syntheses of N-alkylated-carboxamide compounds (3a-3i) were performed by N-C bond formation between methyl (2-oxo-1,2-dihydroquinoline-4-yl)-L-alaninate (**2**) and different alkylating agents (ethane bromide, pentane bromide, hexane bromide, allyl bromide, ethyl acetate bromide, 4-Nitrobenzyl bromide, 2-Bromobenzyl bromide, 2-Methylbenzyl bromide, 3- Bromo-1-phenyl-1-propene bromide).

All the synthesized compounds were purified on a liquid chromatography column using silica gel as a stationary phase and were obtained with good yields ranging from 70% to 90% (Figure 1). The alkylation reactions in both cases showed mono-N-alkylation using 1.2 equivalents, and 2.2 equivalents of alkylating agents reacted only with the nucleophile NH of quinoline. The bond N-C between (**2**) and different alkylating agents was formed for all the synthesized products, and their chemical structures were characterized by ^{1}H and ^{13}C NMR and high-resolution mass spectrometry (ESI-TOFMS).

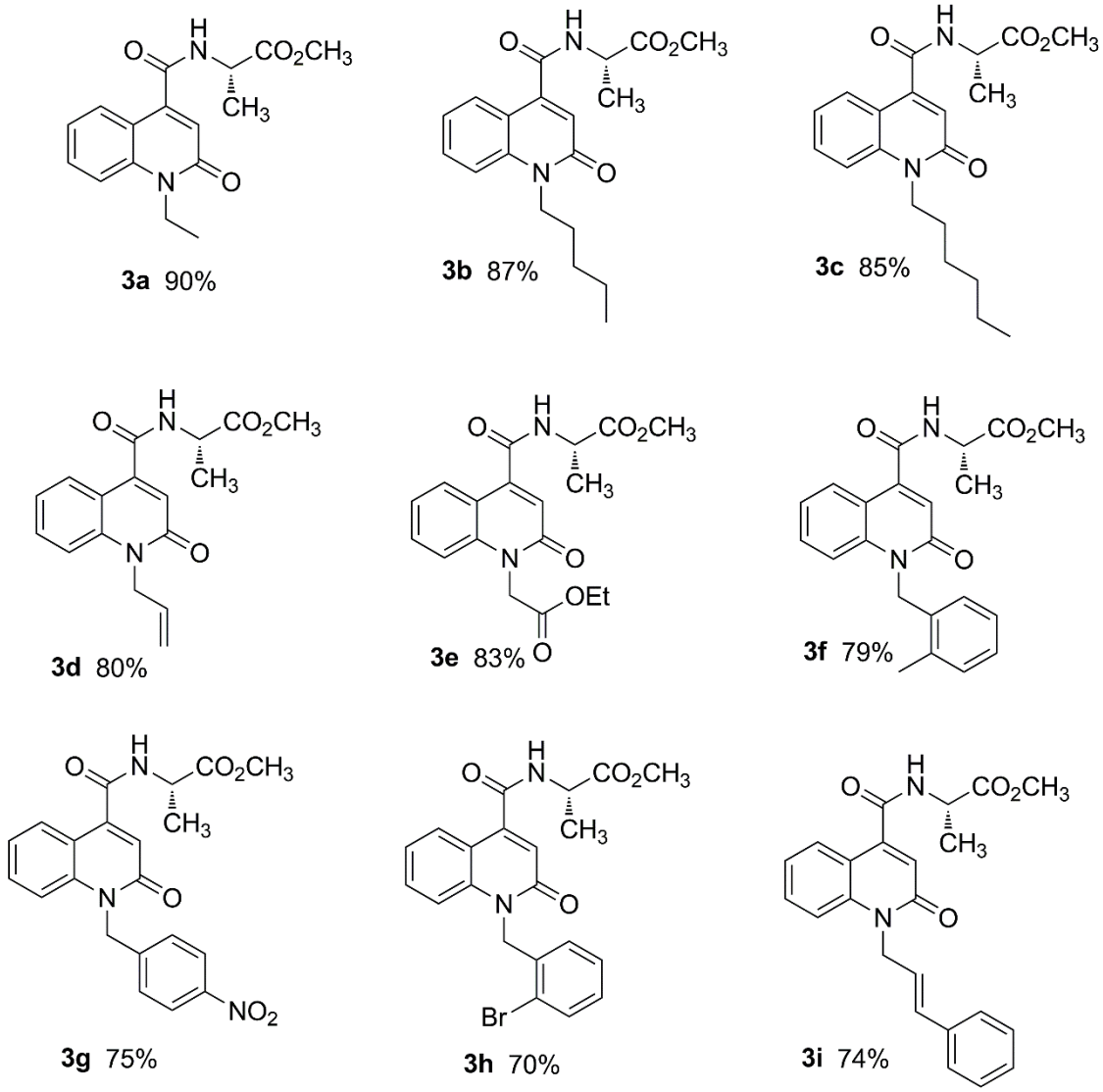


Figure 3. Scoop synthesis of N-alkylated quinolone-carboxamides derivatives (**3a-3i**)

The analysis of the ^{1}H NMR spectra show that the absence of characteristic signals (quinoline proton *NH*) of quinoline-carboxamides derivatives **3a-3i**, the formation of the N-C bond and the presence of doublet with coupling constants ^{3}J correlated to the proton NH of amide, confirming the mono alkylation at the NH of quinoline.

The ^{1}H NMR spectrum of **3a** displayed a triplet, and a doublet at δ=1.28 ppm and δ=1.61 ppm, correspond to CH_3-CH_2 and CH_3-*CH, respectively (Figure 4). The protons of methoxy CH_3-O of ester appear at δ= 3.84 ppm in form intense singlet, two doublets of quadruplet at δ= 4.19 ppm and δ= 4.35 ppm of CH_2-N confirm that tow its protons aren't isochrones, the proton of asymmetric carbon displayed at δ= 4.85 ppm as a doublet of the triplet with two couplings constant ^{3}J= 7.4 Hz and ^{3}J= 7.2 Hz, a singlet at δ= 6.80 ppm correspond to proton ethylenic (H6) of quinolone. The doublet at δ= 7.12 ppm with coupling constant equal ^{3}J= 7,4 Hz illustrates proton amidic NH. The zone between δ= 7.26 ppm to δ= 8 ppm corresponds to aromatic protons.

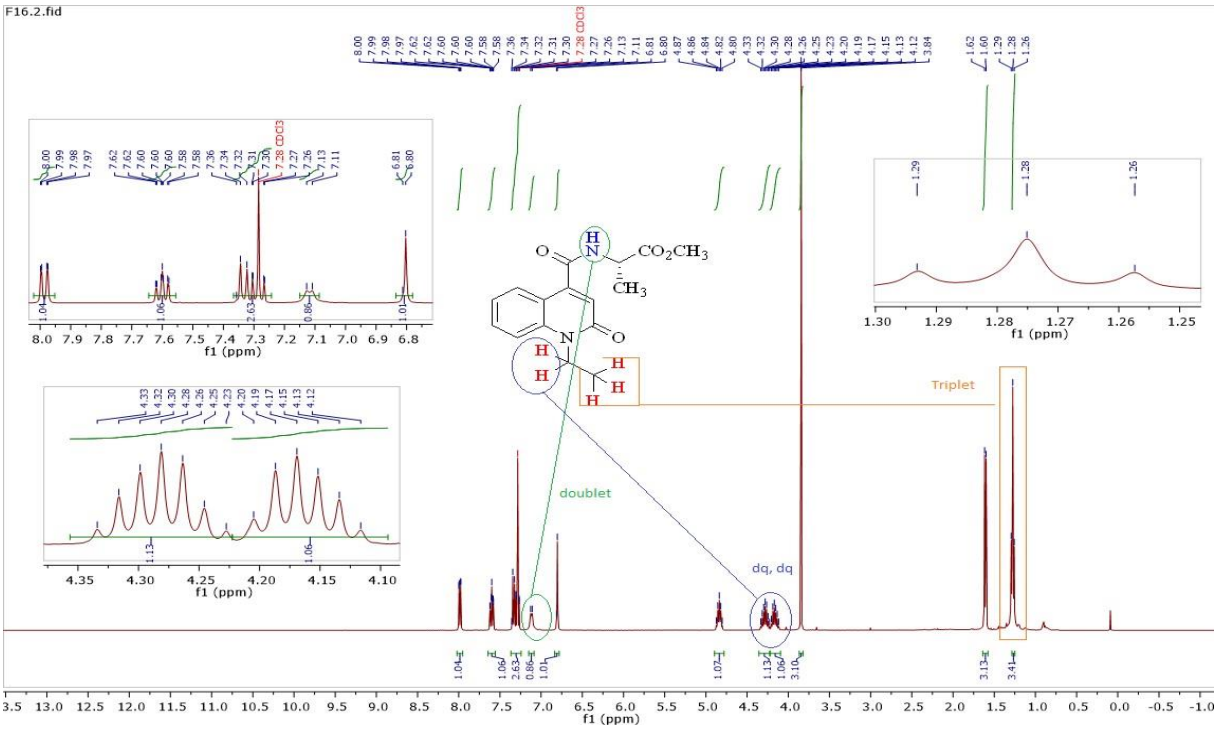
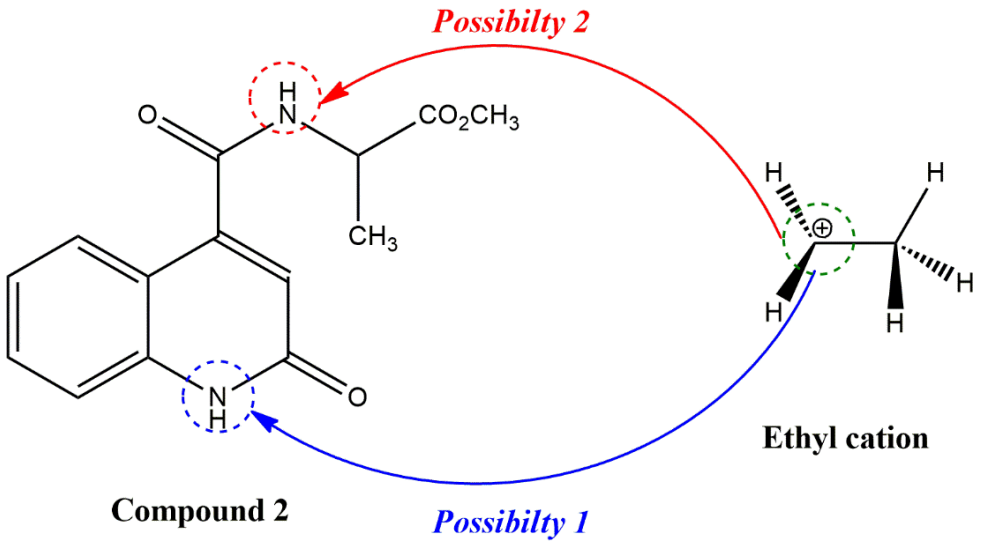


Figure 4. ^{1}H NMR spectrum of compound **3a**

The ^{13}C NMR spectra of all compounds displayed a three deshielded signal correspond to quaternary carbons of amide, amide quinoline, and ester group respectively. For compound 3a, the ^{13}C NMR spectrum presents a signal at δ=172.85 ppm corresponds to the quaternary carbons of amide, the signal of ester carbon appears at 165.06 ppm. At δ=161.00 ppm a signal illustrates the presence of the carbon of quinoline amide. The region between δ=148 to113 ppm assignable to the aromatic carbon. At the same time, the chemical shift of CH_2-N appears at δ(CH_2-N)=37.38 ppm. The shifts of asymmetric carbons *CH-NH, methoxy carbons CH_3-O and primary carbons CH_3 were assigned to their corresponding signals at δ(CH_3)=52, δ=48.54, δ= 37.38, δ=18.08 ppm and δ(CH_3-CH_2)= 12.59 ppm, respectively. Moreover, the mass spectra analysis of compound 3a shows a peak at m/z 325.11 $[M+Na]^+$, which agrees with its molecular formula $C_{16}H_{18}N_2O_4$. The characterizations of all target compounds are presented in the experimental part.

3.2. Mechanistic study

The alkylation reaction of compound (**2**) in the presence of ethyl cation gives two possibilities, as shown in Scheme 2. To get a closer understanding of the chemoselectivity experimentally observed, DFT calculations were performed at the B3LYP/6-311G(d,p) level of both reagents. The optimized geometries obtained and the numbering of the atoms of the most stable conformation of both reactants, the **1a** and ethyl cation, are shown in Figure 4.



Scheme 2. Proposed mechanisms for N-Alkylation reactions of 2 in the presence of ethyl cation

The global reactivity indexes are powerful tools that can explain the reaction mechanism and are measured through the global electron density transfer (GEDT) value [80,81]. In this regard, the global electrophilicity and nucleophilicity indexes of reactants are calculated, and the results are given in Table 1. The results indicate that the bromoethane acts as a moderate electrophile (ω = 1.09 eV) and marginal nucleophile (N = 1.58 eV). The compound 2 as a moderate nucleophile (N = 2.95 eV) and a moderate electrophile (ω = 1.83 eV) within the electrophilicity and nucleophilicity scales. These results confirm that along with this reaction, the bromoethane act as an electrophile and the compound 2 as a nucleophile.

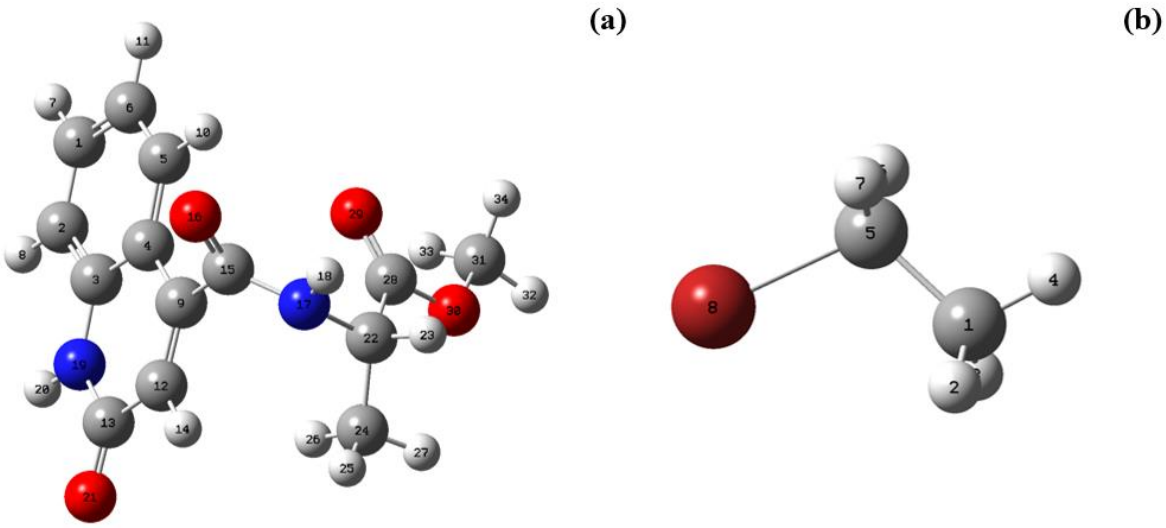


Figure 5. Optimized structures of the compound (**2**) (a) and ethyl cation (b) at B3LYP/6-311G(d,p) level

Table 1. Global reactivity indices of **2** and ethyl cation. Legend: **μ - Electronic chemical potential, η - chemical hardness, ω - global electrophilicity, *N*- global nucleophilicity**

	μ(eV)	**η (eV)**	**ω (eV)**	***N* (eV)**
Compound (2)	-3.99	4.35	1.83	2.95
bromoethane	-3.95	7.18	1.09	1.58

Recently, the Parr functions are used as a helpful tool to explain the regioselectivity and chemoselectivity that are experimentally observed and enable us to distinguish clearly between nucleophilic and electrophilic attacks [82]. The favourable product is associated with the highest P_k^+ Parr function of the electrophile and the highest P_k^- Parr function of the nucleophile. Accordingly, the values of the nucleophilic and electrophilic Parr functions at **2** and bromoethane are calculated and summarized in Figure 6. The nucleophilic P_k^- and electrophilic P_k^+ Parr functions of both reagents were analyzed to study the local reactivity (Figure 6). The nucleophilic P_k^- Parr functions of 2a indicates that the nitrogen N19 with P_k^- the value of 0.18

is more nucleophilically active than the N17 nitrogen atom (P_k^- =0.00). The electrophilic P_k^+ Parr functions of ~~at~~ bromoethane shows that the C5 carbon atom is the most electrophilic center compared with the C1 atom, with P_k^+ values of 0.32 and -0.02, respectively. These results show that the most favorable bond formation will correspond to the N19→C5, leading to the formation of the product **3a** in complete agreement with the chemoselectivity experimentally observed in the alkylation reaction of compound **2**.

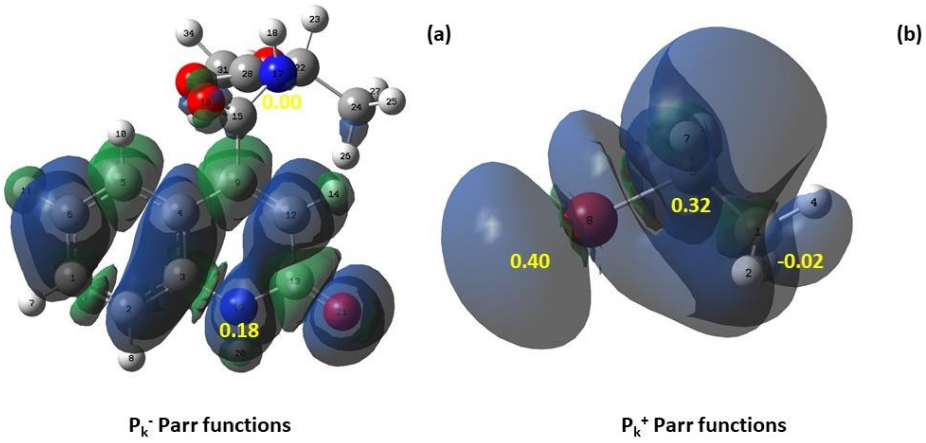


Figure 6. Three-dimensional representation of the Mulliken atomic spin densities of **2** (a) and **bromoethane** (b) together with the Parr functions values.

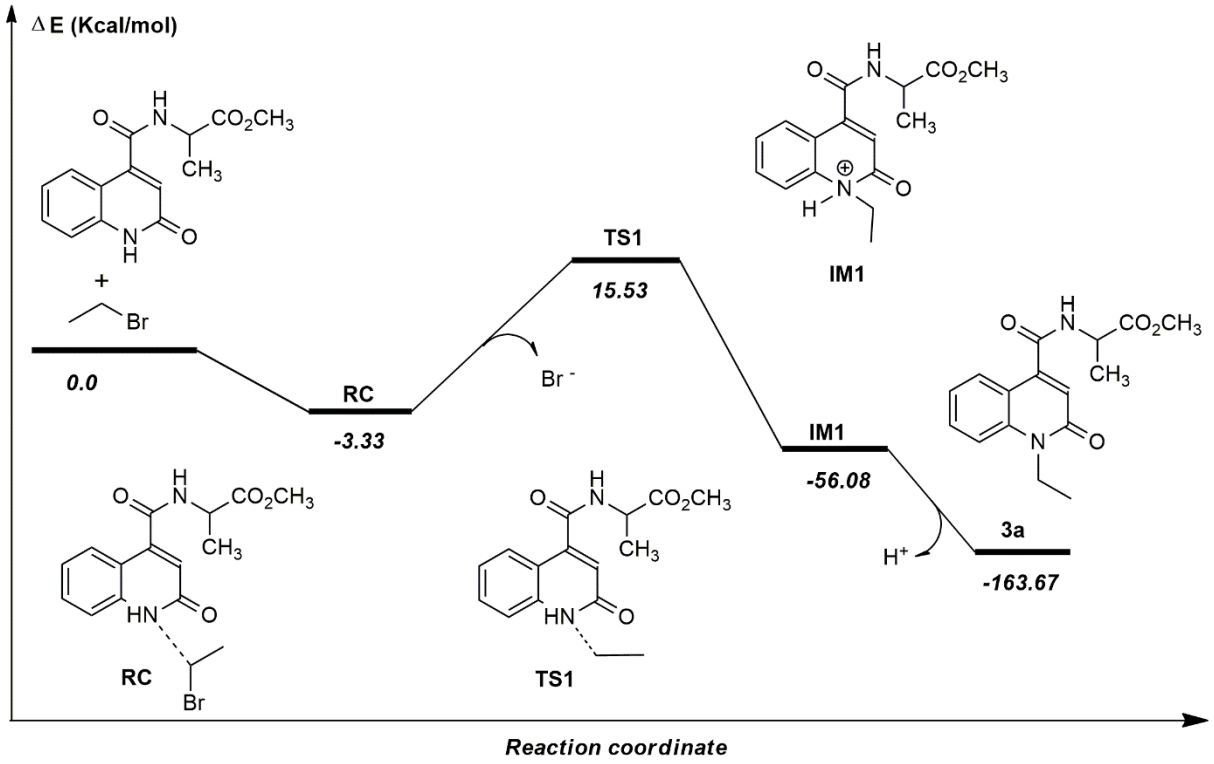


Figure 7. Proposed mechanism for the alkylation of compound **2** in the presence of **bromoethane**

In the first alkylation step of compound **2**, bromoethane binds to the nitrogen atom of the six-membered heterocycle (Figure 7). This coordination conducts to the formation of a reactive complex (RC). This step is exothermic by 3.33 kcal/mol. Then, the elimination of the bromide atom yields to intermediate 1 (IM1) formation through the transition state 1 (TS1). The energetic barrier for this step is 15.53 kcal/mol. Finally, the formation of the product 3a derivative is exothermic by 163.67 kcal/mol. These results allow us to explain the corresponding alkylation product's formation from the compound **3a** (Figure 7).

3.3. Biological activity

The new N-monoalkylated compounds have been screened for their antibacterial activity against *Escherichia coli*, *Staphyloccocus aureus*, *Pseudomonas aeruginosa*, and *Bacillus subtilis*. Besides their antifungal evaluation against *Candida albicans* and *Aspergillus niger*.

Table 2 summarised the result of both the Agar Disc Diffusion Method and microdilution of the antibacterial and antifungal activities of synthesized compounds.

Table 2. Antibacterial and antifungal activities of compound (**3a-3i**).

Bacteria	***Escherichia coli ATCC 25922***	***Staphyloccocus aureus ATCC 29213***	***Pseudomonas aeruginosa ATCC 27853***	***Bacillus subtilis ATCC 3366***	***Candida albicans***	***Aspergillus niger.***
compounds	MIC(ZI)	MIC(ZI)	MIC(ZI)	MIC(ZI)	MIC(ZI)	MIC(ZI)
3a	2.5(10)	0.31(7)	1.25(12)	10(7)	-	10(7)
3b	1.25(9)	0.31(7)	1.25(8)	10(8)	10(8)	10(10)
3c	1.25(5)	0.32(7)	1.25(8)	2.5(9)	-	-
3d	1.25(10)	2.5(10)	1.25(9)	0.62(7)	10(5)	10(7)
3e	0.62(10)	0.31(0)	1.25(10)	10(5)	5(9)	10(7)
3f	1.25(9)	1.25(10)	5(10)	0.31(10)	-	-
3g	0.31(9)	0.078(10)	2.5(10)	5(9)	5(11)	10(9)
3h	2.5(10)	5(10)	0.62(10)	0.0195(12)	10(12)	5(10)
3i	1.25(9)	0.0195 (12)	0.31(10)	0.62(11)	5(9)	10(5)
Ciprofloxacin	15	15	12.5	12.5	-	-
Griseofulvin	-	-	-	-	0.5	0.1

MIC: minimal inhibition concentration (mg/ml)
ZI: zone inhibition (mm)
-: No activity

The majority of compounds tested displayed a good antibacterial than those of the antibiotic reference (Ciproflaxin) and lowest antifungal activity versus the activity of griseofulvin. The compound **3h** was an excellent antibacterial agent against *B. subtilis* with a MIC of 19.5 µg/mL. Similarly, compounds **3e** and **3g** showed better activity against *E. coli* with MICs of 0.62 mg/mL and 0.31 mg/mL, respectively. The compound **3i** showed excellente activity against *S. aureus* with a MIC of 19.5 µg/mL, likewise presented the high activity against *P. aeruginosa* with a MIC of 0.31 mg/mL respectively. Otherwise, a significant antifungal activity with MIC=5 mg/mL was observed for compounds **3e**, **3g**, and **3i** against *C. albicans*, and compound **3h** also acted as moderate antifungal agents against *A. niger* with a high MIC=5 mg/mL than other compounds. Table 2 indicates that the R substituents could also affect the biological

activity of the synthesized compounds (**3a-3i**). Comparing the antibacterial activities of the tested compounds, for R= C_7H_6Br (bromobenzene) substituents shows potent antibacterial activity against *B. subtilis*. In the case of *E. coli*, the R= $C_7H_6NO_2$ (nitrobenzene) substituent has a higher activity than other compounds, possibly due to the presence of bromine groups that play a role in the killing mechanism. The R=C_9H_9 (Propenyl benzene) Whole of allyl and aromatic groups are responsible for the excellent result of antibacterial activity of product **3i** against *S. aureus* and *P. aeruginosa*. The radicals R= C_7H_6Br, $C_7H_6NO_2$ have indicated the antifungal activity of the corresponding compounds against *A. niger*; similarly, the radical R=$C_4H_7O_2$ (ethyl acetate) appeared the high antifungal activity against *C. albicans* than other radicals.

3.4. Molecular Docking

After the docking procedure, we classified the ligands based on their docking scores. The following table shows the results of the docking with Glide (Table 3).

Table 3. Docking score and Lipinski's rule of the compounds

Ligand	Docking score (kcal/mol)	Lipinski rule of five			
3c	**-10.415**	MW=358,43	LogP=4,84	H-bond donors= 1	H-bond acceptors=4 PSA=77,4
3g	**-9.558**	MW=409,39	LogP=3,65	H-bond donors= 1	H-bond acceptors=4 PSA=77,4
3h	**-9.504**	MW=409,39	LogP=3,08	H-bond donors= 1	H-bond acceptors=4 PSA=120,5
3i	**-10,141**	MW=443,29	LogP=3,93	H-bond donors= 1	H-bond acceptors=4 PSA=77,4

3c to 3g are the compounds name**, Mw** is Molecular wheat**, PSA** is Polar surface area.

After aligning the ligands in the protein binding site, we find that all ligands bind to the same region of the binding pocket using the same mechanism, as shown in Figure 8 below.

Compound **3c** has a docking score of -10.41, which is the lowest among all compounds, then compound **3i** with a score of -10.14, **3g** with -9.55 and **3h** with -9.50.

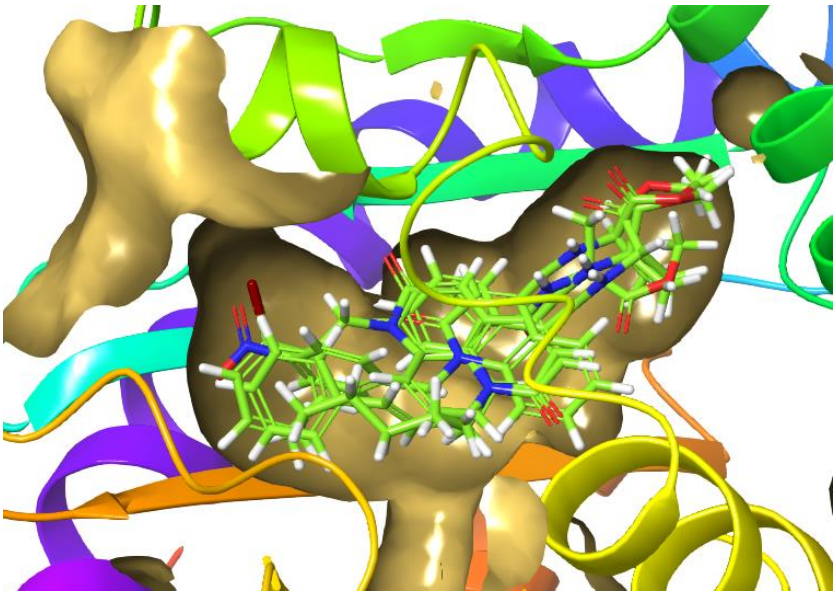


Figure 8. 3D interaction of the compounds (**3c**, **3g**, **3h** and **3i**) in the binding site of the LasR protein.

Regarding this binding mechanism, we decided to study the interaction between the ligands and the amino acids present in the protein binding pocket and assess the type of bond formed in the complexes (3c, 3g, 3h, 3i) (see Figure 9).

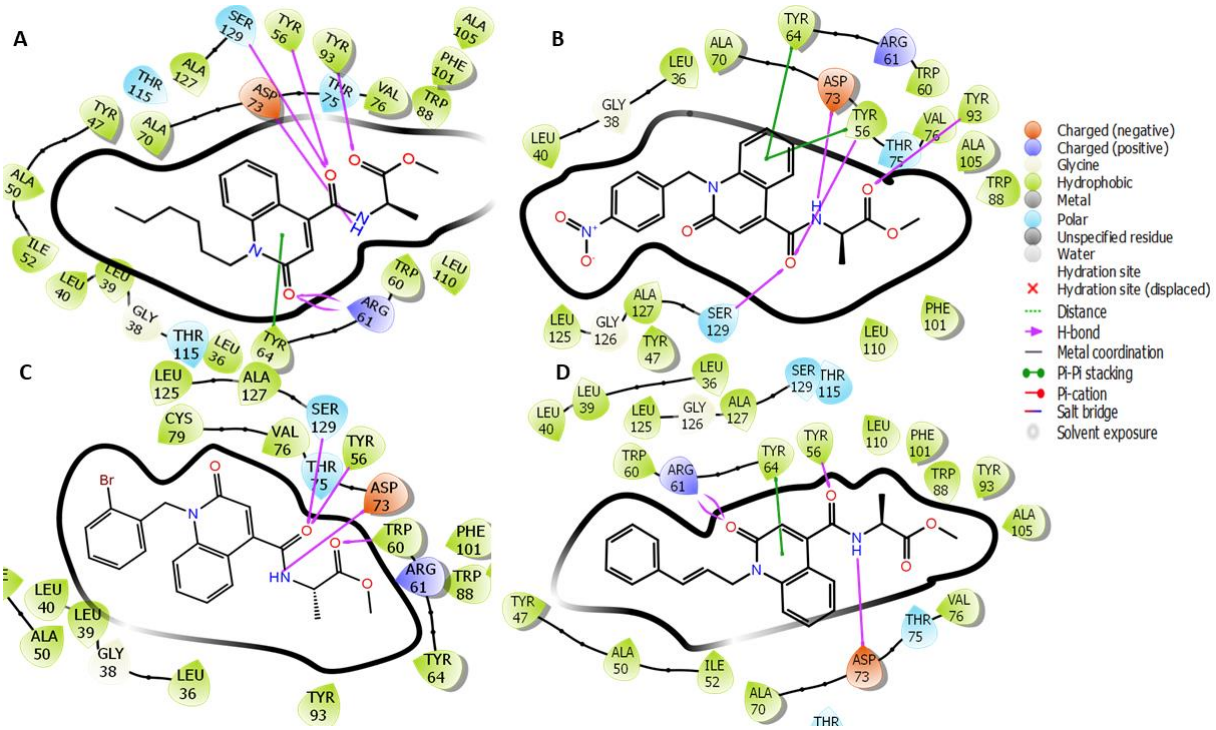


Figure 9. 2D interaction of **3c** (A), **3g** (B), **3h** (C) and **3i** (D) compounds in the binding site of the LasR protein

We have observed that the side chain residues TYR56, ARG61, TYR93, and SER129 form hydrogen bonds as a donor with the carbonyl groups present in compound 3c, while ASP37 forms hydrogen bonds as an acceptor with the nitrogen-bonded hydrogen atom and a two π-π stacking interaction between TYR64 and the pyridone ring. In the case of compound 3g, the side chain residues TYR56, TYR93, and SER129 form donor hydrogen bonds with the carbonyl group of compound B, while ASP37 accepts hydrogen bonds from the hydrogen atom of the amide group, and two π-π stacking interactions of quinoline with TYR56 and TYR 64 are formed. In compound **3h**, the side chain residues TYR56, TRP60, and SER129 act as hydrogen bond donors with the NH-separated oxide group, and ASP73 forms hydrogen bond acceptors with the NH group.

In the last example (compound **3i**), the side chain residues TYR56, ARG61, and ASP73 form hydrogen bonds with two carbonyl groups separated by quinoline TYR64 forms a π-π interaction with the quinoline group.

3.4. Molecular dynamics

The compound **3h**, which has the lowest docking score and the highest experimental activity, has been selected for further analysis, giving the atoms more degrees of freedom with molecular dynamics to analyze and examine the stability of the complex formed by our ligand (**3h**) and the protein with the Yasara software (Figure 10).

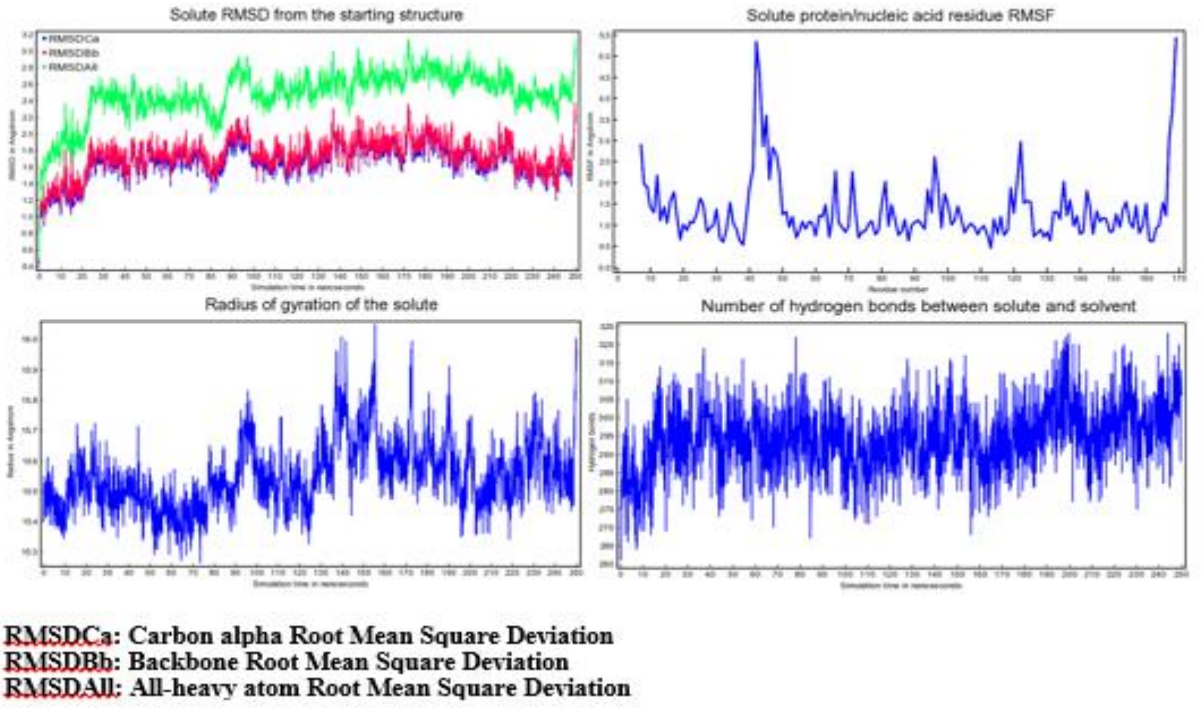


Figure 10. The MD trajectory analysis for the complex between LaS and inhibitor 3h. Legend: The RMSD (top left), Radius of gyration (bottom left), RMSF (top right) of the protein-inhibitor complex and number of Hydrogen Bonds formed between the complex and solvent (bottom right).

From the trajectory analysis, we can observe relatively low values of the solute RMSD from the starting point; for example, the average value of the α-carbon atom RMSD is 1.6 Å, indicating the stability of the complex between LaS protein and the inhibitor.

The gyration (Rg) radius was calculated to understand the degree of compaction in the ligand's LasR protein structure. The gyration radius (Rg) was calculated to understand the compaction's degree in the complex between the LasR protein and its inhibitor. The Rg is defined as the root mean square distance of the collection of atoms from their common centroid. Note that the stable protein complex has a compact gyration radius of no more than 22 Å [83]. Root mean square fluctuation (RMSF) describes how much a given residue moves (fluctuates) during a simulation. RMSF plot indicates which amino acids in a protein contribute the most to molecular motion.

The hydrogen bond network's stability formed between the LasR protein and the solvent was measured for the ligated system at 300 K in the simulation. We found an average of 295 hydrogen bonds between the solute and the solvent during 250 ns, and this value is nearly stable during the simulation, indicating the complex's stability.

4. Conclusion

In summary, a new derivative of N-alkylated methyl-(2-oxo-1,2-dihydroquinoline-4-yl)-L-alaninate derivatives (**3a-3i**) was synthesized by substituting methyl-(2-oxo-1,2-dihydroquinolin-4-yl)-L-alaninate and various types of alkylating agents including alkane, alkene, aromatics, and ester groups via an N-alkylation reaction using TBAB as a transfer catalyst. All synthesized products were purified and characterized by ^{1}H- and ^{13}C-NMR and ESI-TOF mass spectrometry. The reactions were carried out at one site of the quinolone (NH of quinoline); this result was confirmed by a theoretical study with DFT calculation, proving that NH of quinolone (lactam) has a stronger nucleophilicity than NH of amide. The novel N-

monoalkylated pharmacophores have shown good antibacterial activity against *Escherichia coli*, *Staphylococcus aureus*, *Pseudomonas aeruginosa*, and *Bacillus subtilis*, the compounds **3h** and **3i** showed the high activities against *Staphylococcus aureus* and *Bacillus subtilis* respectively with MIC=19.5 µg/mL. Moreover, most of the compounds showed moderate antifungal activity against *Candida albicans* and *Aspergillus niger* with MIC ranging from 10 mg/mL to 5 mg/mL Molecular docking was used to classify the in-silico activity of the compounds and to predict the best binding conformation to the LasR protein. In contrast, molecular dynamics was used to study the stability of the complex formed in the cellular environment, including other elements such as H_2O, NaCl. These two techniques confirmed the experimental results of the antibacterial activities of our compounds.

Supplementary material: Supplementary File

Acknowledgements: The authors would like to thank Chemistry University from Helsinki, Finland, and Chouaib Doukkali University, Morocco. Special thanks are also due to Hassan Haddad. A big thanks go to Prof. Abdeltif Boukir and Prof. Abdeslem Bentama for their continuous support and guidance in the following years, which motivated me to write and edit this article.

Author Contributions: Conceptualization: OM and LB; methodology, LB, MEH, SB, CP, computational analysis, LB, MEH and AA; structural analysis, OM, KM and RS; antibacterial activity, OM; resources, EE, SC and EE; writing-original draft preparation, OM, SC and LB; writing-review and editing, KM, SC, EE, LB, MEH and CP; supervision, SC and EE; supervision of computational modelling, LB and MEH. All authors have read and agreed to the published version of the manuscript.

Conflicts of Interest: The authors declare no conflict of interest.

References

[1] E.A. Ashley, M. Dhorda, R.M. Fairhurst, C. Amaratunga, P. Lim, S. Suon, S. Sreng, J.M. Anderson, S. Mao, B. Sam, C. Sopha, C.M. Chuor, C. Nguon, S. Sovannaroth, S. Pukrittayakamee, P. Jittamala, K. Chotivanich, K. Chutasmit, C. Suchatsoonthorn, R. Runcharoen, T.T. Hien, N.T. Thuy-Nhien, N.V. Thanh, N.H. Phu, Y. Htut, K.-T. Han, K.H. Aye, O.A. Mokuolu, R.R. Olaosebikan, O.O. Folaranmi, M. Mayxay, M. Khanthavong, B. Hongvanthong, P.N. Newton, M.A. Onyamboko, C.I. Fanello, A.K. Tshefu, N. Mishra, N. Valecha, A.P. Phyo, F. Nosten, P. Yi, R. Tripura, S. Borrmann, M. Bashraheil, J. Peshu, M.A. Faiz, A. Ghose, M.A. Hossain, R. Samad, M.R. Rahman, M.M. Hasan, A. Islam, O. Miotto, R. Amato, B. MacInnis, J. Stalker, D.P. Kwiatkowski, Z. Bozdech, A. Jeeyapant, P.Y. Cheah, T. Sakulthaew, J. Chalk, B. Intharabut, K. Silamut,,S.J. Lee, B. Vihokhern, C. Kunasol, M. Imwong, J. Tarning, W.J. Taylor, S. Yeung, C.J. Woodrow, J.A. Flegg, D. Das, J. Smith, M. Venkatesan, C.V. Plowe, K. Stepniewska, P.J. Guerin, A.M. Dondorp, N.P. Day, N.J. White, Tracking Resistance to Artemisinin Collaboration (TRAC), Spread of artemisinin resistance in Plasmodium falciparum malaria, N Engl J Med. 371 (2014) 411–423.

[2] E. Tacconelli, E. Carrara, A. Savoldi, S. Harbarth, M. Mendelson, D.L. Monnet, C. Pulcini, G. Kahlmeter, J. Kluytmans, Y. Carmeli, M. Ouellette, K. Outterson, J. Patel, M. Cavaleri,
E.M. Cox, et al, Discovery, research, and development of new antibiotics: The WHO priority list of antibiotic-resistant bacteria and tuberculosis. Lancet Infect, Dis. 18 (2018) 318–327.

[3] J. Lee, L. Zhang,. The hierarchy quorum sensing network in Pseudomonas aeruginosa, Protein Cell. 6 (2015) 26–41.

[4] M. Pérez-Pérez, P. Jorge, G. Pérez Rodríguez, M.O. Pereira, A. Lourenço,. Quorum sensing inhibition in Pseudomonas aeruginosa biofilms: New insights through network mining, Biofouling. 33 (2017) 128–142.

[5] P. Williams, M. Cámara,. Quorum sensing and environmental adaptation in Pseudomonas aeruginosa: Atale of regulatory networks and multifunctional signal molecules, Curr. Opin. Microbiol. 12 (2009) 182–191.

[6] S.T. Rutherford, B.L. Bassler,. Bacterial quorum sensing: its role in virulence and possibilities for its control, Cold Spring Harb Perspect. Med. 2 (2012) a012427.

[7] A. Marella, O.P. Tanwar, R. Saha, M.R. Ali, S. Srivastava, M. Akhter, M. Shaquiquzzaman, M.M. Alam, Quinoline: A versatile heterocyclic, Saudi Pharmaceutical Journal. 21 (2013) 1–12. https://doi.org/10.1016/j.jsps.2012.03.002.

[8] J. Achan, A.O. Talisuna, A. Erhart, A. Yeka, J.K. Tibenderana, F.N. Baliraine, P.J. Rosenthal, U. D'Alessandro, Quinine, an old anti-malarial drug in a modern world: role in the treatment of malaria, Malaria Journal. 10 (2011) 144. https://doi.org/10.1186/1475- 2875-10-144.

[9] S. Eswaran, A.V. Adhikari, N.S. Shetty, synthesis and antimicrobial activities of novel quinoline derivatives carrying 1,2,4-triazole moiety, European Journal of Medicinal Chemistry. 44 (2009) 4637–4647.

[10] F. Pierre, S.E. O'Brien, M. Haddach, P. Bourbon, M.K. Schwaebe, E. Stefan, L. Darjania, R. Stansfield, C. Ho, A. Siddiqui-Jain, N. Streiner, W.G. Rice, K. Anderes, D.M. Ryckman, Novel potent pyrimido[4,5-c]quinoline inhibitors of protein kinase CK2: SAR and preliminary assessment of their analgesic and anti-viral properties, Bioorganic & Medicinal Chemistry Letters. 21 (2011) 1687–1691.

[11] K.D. Thomas, A.V. Adhikari, N.S. Shetty, design, synthesis and antimicrobial activities of some new quinoline derivatives carrying 1,2,3-triazole moiety, European Journal of Medicinal Chemistry. 45 (2010) 3803–3810.

[12] S. Xy, W. Cx, C. Ky, P. Hr, Q. Zs, Synthesis and anti-inflammatory activity evaluation of novel 7-alkoxy-1-amino-4,5-dihydro[1,2,4]triazole[4,3-a]quinolines.,

Arch Pharm (Weinheim). 341 (2008) 288–293.
[13] S.I. Pretorius, W.J. Breytenbach, C. de Kock, P.J. Smith, D.D. N'Da, synthesis, characterization and antimalarial activity of quinoline-pyrimidine hybrids, Bioorg Med Chem. 21 (2013) 269–277.
[14] G. Roma, G. Grossi, M. Di Braccio, D. Piras, V. Ballabeni, M. Tognolini, S. Bertoni, E. Barocelli, 1,8-Naphthyridines VII. New substituted 5-amino[1,2,4]triazolo[4,3-a][1,8]naphthyridine-6-carboxamides and their isosteric analogues, exhibiting notable anti-inflammatory and/or analgesic activities, but no acute gastrolesivity, European Journal of Medicinal Chemistry. 43 (2008) 1665–1680.
[15] M.C. Mandewale, U.C. Patil, S.V. Shedge, U.R. Dappadwad, R.S. Yamgar, A review on quinoline hydrazone derivatives as a new class of potent antitubercular and anticancer agents, Beni-Suef University Journal of Basic and Applied Sciences. 6 (2017) 354–361. https://doi.org/10.1016/j.bjbas.2017.07.005.
[16] N. Suresh, H.N. Nagesh, J. Renuka, V. Rajput, R. Sharma, I.A. Khan, C.S. Kondapalli Venkata Gowri, Synthesis and evaluation of 1-cyclopropyl-6-fluoro-1,4-dihydro-4-oxo- 7-(4-(2-(4-substitutedpiperazin-1-yl)acetyl)piperazin-1-yl)quinoline-3-carboxylic acid derivatives as anti-tubercular and antibacterial agents, Eur J Med Chem. 71 (2014) 324– 332.
[17] X. Bu, J. Chen, L.W. Deady, C.L. Smith, B.C. Baguley, D. Greenhalgh, S. Yang, W.A. Denny, Synthesis and cytotoxic activity of N-[(alkylamino)alkyl]carboxamide derivatives of 7-oxo-7H-benz[de]anthracene, 7-oxo-7H-naphtho[1,2,3-de]quinoline, and 7-oxo-7H- benzo[e]perimidine, Bioorganic & Medicinal Chemistry. 13 (2005) 3657–3665.
[18] B. Chakraborty, D. Dutta, S. Mukherjee, S. Das, N.C. Maiti, P. Das, C. Chowdhury, Synthesis and biological evaluation of a novel betulinic acid derivative as an inducer of apoptosis in human colon carcinoma cells (HT-29), Eur J Med Chem. 102 (2015) 93–105.
[19] I. Tomassoli, L. Ismaili, M. Pudlo, C. de los Ríos, E. Soriano, I. Colmena, L. Gandía, L. Rivas, A. Samadi, J. Marco-Contelles, B. Refouvelet, Synthesis, biological assessment and molecular modeling of new dihydroquinoline-3-carboxamides and dihydroquinoline- 3-carbohydrazide derivatives as cholinesterase inhibitors, and Ca channel antagonists, European Journal of Medicinal Chemistry. 46 (2011) 1–10.
[20] Y. Filali Baba, Y. Sert, Y. Kandri Rodi, S. Hayani, J.T. Mague, D. Prim, J. Marrot, F. Ouazzani Chahdi, N.K. Sebbar, E.M. Essassi, Synthesis, crystal structure, spectroscopic characterization, Hirshfeld surface analysis, molecular docking studies and DFT calculations, and antioxidant activity of 2-oxo-1,2-dihydroquinoline-4-carboxylate derivatives, Journal of Molecular Structure. 1188 (2019) 255–268.
[21] N. Okamura, T. Suemoto, S. Furumoto, M. Suzuki, H. Shimadzu, H. Akatsu, T. Yamamoto, H. Fujiwara, M. Nemoto, M. Maruyama, H. Arai, K. Yanai, T. Sawada, Y. Kudo, Quinoline and benzimidazole derivatives: candidate probes for in vivo imaging of tau pathology in Alzheimer's disease, J Neurosci. 25 (2005) 10857–10862.
[22] P. Hochegger, J. Faist, W. Seebacher, R. Saf, P. Mäser, M. Kaiser, R. Weis, Synthesis and structure-activity relationships for new 6-fluoroquinoline derivatives with antiplasmodial activity, Bioorganic & Medicinal Chemistry. 27 (2019) 2052–2065.
[23] M. Rbaa, S. Jabli, Y. Lakhrissi, M. Ouhssine, F. Almalki, T. Ben Hadda, S. Messgo-Moumene, A. Zarrouk, B. Lakhrissi, Synthesis, antibacterial properties and bioinformatics computational analyses of novel 8-hydroxyquinoline derivatives, Heliyon. 5 (2019) e02689.

[24] J.D. Bilavendran, A. Manikandan, P. Thangarasu, K. Sivakumar, Synthesis and biological activities of nitro-hydroxy-phenylquinolines; validation of antibiotics effect over DNA gyrase inhibition and antimicrobial activity, Journal of Heterocyclic Chemistry. 57 (2020) 1143–1153.
[25] I. Sorribes, J.R. Cabrero-Antonino, C. Vicent, K. Junge, M. Beller, Catalytic N-Alkylation of Amines Using Carboxylic Acids and Molecular Hydrogen, J. Am. Chem. Soc. 137 (2015) 13580–13587.
[26] M.J. Nieves-Remacha, M. Torres, M. Ruiz-Abad, J.A. Rincón, G.R. Cumming, P. Garcia- Losada, Scale-up of N-alkylation reaction using phase-transfer catalysis with integrated separation in flow, React. Chem. Eng. 4 (2019) 334–345.
[27] O. Moussaoui, R. Bhadane, R. Sghyar, E.M. El Hadrami, S. El Amrani, A. Ben Tama, Y. Kandri Rodi, S. Chakroune, O.M.H. Salo-Ahen, Novel Amino Acid Derivatives of Quinolines as Potential Antibacterial and Fluorophore Agents. Sci. Pharm. 88 (2020) 57.
[28] M. Subaramanian, S.P. Midya, P.M. Ramar, E. Balaraman, General Synthesis of N-Alkylation of Amines with Secondary Alcohols via Hydrogen Autotransfer, Org. Lett. 21 (2019) 8899–8903.
[29] J.T. Madak, C.R. Cuthbertson, Y. Miyata, S. Tamura, E.M. Petrunak, J.A. Stuckey, Y. Han, M. He, D. Sun, H.D. Showalter, N. Neamati, Design, Synthesis, and Biological Evaluation of 4-Quinoline Carboxylic Acids as Inhibitors of Dihydroorotate Dehydrogenase, J. Med. Chem. 61 (2018) 5162–5186.
[30] Y. Ling, QX. Yang, YN. Teng, S. Chen, WJ. Gao, J. Guo, PL. Hsu, Y. Liu, SL. Morris- Natschke, CC. Hung, KH. Lee, Development of novel amino-quinoline-5,8-dione derivatives as NAD(P)H:quinone oxidoreductase 1 (NQO1) inhibitors with potent antiproliferative activities. Eur J Med Chem. 154 (2018) 199-209.
[31] K.D. Katariya, S.R. Shah, D. Reddy, Anticancer, antimicrobial activities of quinoline based hydrazone analogues: Synthesis, characterization and molecular docking, Bioorganic Chemistry. 94 (2020) 103406.
[32] J. Mo, H. Yang, T. Chen, Q. Li, H. Lin, F. Feng, W. Liu, W. Qu, Q. Guo, H. Chi, Y. Chen,
H. Sun, Design, synthesis, biological evaluation, and molecular modeling studies of quinoline-ferulic acid hybrids as cholinesterase inhibitors, Bioorganic Chemistry. 93 (2019) 103310.
[33] O. Moussaoui, E.M.E. Hadrami, G.B. Touimi, B. Bennani, A.B. Tama, S. Chakroune, A. Boukir, Synthesis of a new serie of quinoline-carboxamides based on methylated aminoesters: NMR characterization and antimicrobial activity, Mediterr. J. Chem. 9 (2019) 326–336.
[34] K. Arya, M. Agarwal, Microwave prompted multigram synthesis, structural determination, and photo-antiproliferative activity of fluorinated 4-hydroxyquinolinones, Bioorg Med Chem Lett. 17 (2007) 86-93.
[35] K. Tsuji, G. Spears, K. Nakamura, T. Tojo, N. Seki, A. Sugiyama, M. Matsuo. Quinoline- 3-carbothioamides and related compounds as novel immunomodulating agents, Bioorg. Med. Chem. Lett. 12 (2002) 2427-30.
[36] A. Kumar, J. Fernandes, P. Kumar, Synthesis, antimicrobial and antitubercular activities of some novel carboxamide derivatives of 2-quinolones, Orient. J. Chem. 4 (2014) 1993– 1997.
[37] P.K. Patel, R.V. Patel, D.H. Mahajan, P.A. Parikh, G.N. Mehta, C. Pannecouque, E. De Clercq, K.H. Chikhalia, different heterocycles functionalized s-triazine analogues: design, synthesis and in vitro antimicrobial, antituberculosis, and anti-hiv assessment, J. Heterocycl. Chem. 51 (2014) 1641–1658.

[38] W. Xue, X. Li, G. Ma, H. Zhang, Y. Chen, J. Kirchmair, J. Xia, S. Wu, Nthiadiazole-4- hydroxy-2-quinolone-3-carboxamides bearing heteroaromatic rings as novel antibacterial agents: Design, synthesis, biological evaluation and targeidentification, European Journal of Medicinal Chemistry (2020).
[39] T. Li, X. LiComprehensive mass analysis for chemical processes, a case study on L-Dopa manufacture, Green Chem. 16 (2014) 4241-4256
[40] T. Nagasaki, M. Sugita, K. Nakagawa, H. Koyaema, Process for the manufacture of 3,4- disubstituted phenyl-L-alanines. Patent US3767528 1973.
[41] A. Torrado, B. ImperialiNew synthetic amino acids for the design and synthesis of peptide- based metal ion sensors, J. Organomet. Chem. 61 (1996) 8940-8948.
[42] M.K. Sinha, K. Khoury, E. Herdtweck, A. DömlingTricycles by a new Ugi variation and Pictet–Spengler reaction in one pot, Chem. Eur. J. 19 (2013) 8048-8052.
[43] K. Ishihara, M. FushimiDesign of a small-molecule catalyst using intramolecular cation- π interactions for enantioselective Diels-Alder and Mukaiyama-Michael reactions: L- DOPA-derived monopeptide, Cu(II) complex, Org. Lett. 8 (2006) 1921-1924.
[44] R.C. Nangreave, L.M. Dedkova, S. Chen, S.M. HechtA new strategy for the synthesis of bisaminoacylated tRNAs, Org. Lett. 13 (2011) 4906-4909.
[45] O. Bassas, N. Llor, M.M.M. Santos, R. Griera, E. Molins, M. Amat, J. BoschBiogenetically inspired enantioselective approach to indolo [2,3-a]- and benzo[a]quinolizidine alkaloids from a synthetic equivalent of secologanin, Org. Lett. 7 (2005) 2817-2820.
[46] N.J. O'Rreilly, W.S. Derwin, H.C. Lin Optically pure (S)-6,7-dimethoxy-1,2,3,4 tetrahydro-3-isoquinolinecarboxylic acid and asymmetric hydrogenation studies related to its preparation, Synthesis-Stuttgart. 7 (1990) 550-556
[47] T.R. Julian and W.L. Jorgensen. "Performance of B3LYP density functional methods for a large set of organic molecules." Journal of Chemical Theory and Computation 4.2 (2008): 297-306.
[48] M.J. Frisch, et al., Gaussian 09, Gaussian Inc, Wallingford CT, 2009.
[49] G. Singh, R. Sachdeva, B. Rai, G.S.S. Saini, structure and vibrational spectroscopic study of alpha-tocopherol, J. Mol. Struct. 1144 (2017) 347–354.
[50] M. E. Hachim, K. Sadik, S. Byadi, C. Van Alsenoy & A. Aboulmouhajir, Ab initio study on the six lowest energy conformers of iso-octane: conformational stability, barriers to internal rotation, natural bond orbital and first-order hyperpolarizability analyses, UV and NMR predictions, spectral temperature sensitivity, and scaled vibrational assignment. Journal of molecular modeling, (2019) 25(8), 1-19.
[51] M. E. Hachim, K. Sadik, S. Byadi & A. Aboulmouhajir. Electronic investigation and spectroscopic analysis using DFT with the long-range dispersion correction on the six lowest conformers of 2.2. 3-trimethyl pentane. Journal of Molecular Modeling, (2020) 26, 1-16.
[52] P. Geerlings, F. De Proft, W. Langenaeker, Conceptual Density Functional Theory, Chem. Rev. 103 (2003) 1793–1874.
[53] L.R. Domingo, M. Ríos-Gutiérrez, P. Pérez, Applications of the Conceptual Density Functional Theory Indices to Organic Chemistry Reactivity, Molecules. 21 (2016).
[54] L. R. Domingo, A new C–C bond formation model based on the quantum chemical topology of electron density, RSC Advances. 4 (2014) 32415–32428.
[55] L.R. Domingo, P. Pérez, J.A. Sáez, Understanding the local reactivity in polar organic reactions through electrophilic and nucleophilic Parr functions, RSC Adv. 3 (2013) 1486– 1494.

[56] K. Sadik, NE. Hamdani, M.E. Hachim, S. Byadi, I. Bahadur & A. Aboulmouhajir. Towards a theoretical understanding of alkaloid-extract Cytisine derivatives of Retama monosperma (L.) Boiss. Seeds, as eco-friendly inhibitor for carbon steel corrosion in acidic 1M HCl solution. Journal of Theoretical and Computational Chemistry, (2020) 19 (05), 2050013.

[57] M. E. Hachim, A. Oubella, S. Byadi, M. Fawzi, Y. Laamari, L. Bahsis et al. Newly synthesized (R)-carvone-derived 1, 2, 3-triazoles: structural, mechanistic, cytotoxic and molecular docking studies. Journal of Biomolecular Structure and Dynamics, (2021) 1-14. doi: 10.1080/07391102.2021.1894984.

[58] MRS Zaidan, A. Noor Rain, AR. Badrul, A. Adlin, A. Norazah, I. Zakiah, In vitro screening of five local medicinal plants for antibacterial activity using disc diffusion method, Trop. Biomed. 22 (2005) 165-170.

[59] D.F. Basri, C.K. Luoi, A.M. Azmi, J. Latip, Evaluation of the Combined Effects of Stilbenoid from Shorea gibbosa and Vancomycin against Methicillin-Resistant Staphylococcus aureus (MRSA). Pharmaceuticals, 5 (2012) 1032–1043.

[60] W. Ouedrhiri, S. Bouhdid, M. Balouiri, A.E.O. Lalami, S. Moja, F.O. Chahdi, H. Greche. Chemical composition of Citrus aurantium L. leaves and zest essential oils, their antioxidant, antibacterial single and combined effects. Journal of Chemical and Pharmaceutical Research, 7 (2015) 78-84.

[61] Q. Sensing, Quorum Sensing and Bacterial Social Interactions in Biofilms, (2012) 2519– 2538.

[62] H.O. Sintim, L. Yan, Paradigm shift in discovering next-generation anti-infective agents : targeting quorum sensing , c-di-GMP signaling and biofilm formation in bacteria with small molecules, 2 (2010) 1005–1035.

[63] A.E. Clatworthy, E. Pierson, D.T. Hung, Targeting virulence : a new paradigm for antimicrobial therapy, 3 (2007) 541–548.

[64] R.A. Friesner, J.L. Banks, R.B. Murphy, Glide: A New Approach for Rapid, Accurate Docking and Scoring. 2. Enrichment Factors in Database Screening, J. Med. Chem. 47 (2004) 1739–1749..

[65] J.W. Costerton, Cystic fibrosis pathogenesis and the role of biofilms in persistent infection. 9 (2001) 50–52.

[66] J.B. Lyczak, C.L. Cannon, G.B. Pier, Establishment of Pseudomonas aeruginosa infection : lessons from a versatile opportunist, (2000) 1051–1060.

[67] T. Praneenararat, G.D. Geske, H.E. Blackwell, Efficient Synthesis and Evaluation of Quorum-Sensing Modulators Using Small Molecule Macroarrays, (2009) 2007–2010.

[68] W.R.J.D. Galloway, J.T. Hodgkinson, M. Welch, D.R. Spring, Previews Mastering the Chemical Language of Bacteria, Chemistry & Biology, 16 (2009) 913–914.

[69] G.D. Geske, R.J. Wezeman, A.P. Siegel, H.E. Blackwell, Small Molecule Inhibitors of Bacterial Quorum Sensing and Biofilm Formation, 2 (2005) 12762–12763.

[70] Berman, HM, Westbrook, J, Feng, Z, Gilliland, G, Bhat, TN, Weissig, H, Shindyal ov, IN, Bourne, PE. The Protein Data Bank, 1999-. In: International Tables for Crystallography volume F: Crystallography of biological macromolecules. Springer Netherlands. (2006) 675–684.

[71] Krieger, E., Dunbrack, R., Hooft, R., & Krieger, B. (2012). Assignment of protonation states in proteins and ligands: Combining pKa prediction with hydrogen bonding network optimization. Methods in Molecular Biology, 819, 405–421. https://doi.org/10.1007/978-1-61779-465-0

[72] D.A. Case, T.E. Cheatham, III, T. Darden, H. Gohlke, R. Luo, K.M. Merz, Jr., A. Onufriev, C. Simmerling, B. Wang and R. Woods. The Amber biomolecular

simulation programs. J. Computat. Chem. 26, 1668-1688 (2005).
[73] W. L. Jorgensen, J. Chandrasekhar, J. D. Madura, R. W. Impey and M. L. Klein, J. Comparison of simple potential functions for simulating liquid water Chem. Phys., 1983, 79, 926-935.
[74] A. Jakalian, DB. Jack, CI. .Bayly Fast, efficient generation of high-quality atomic charges. AM1-BCC model: II. Parameterization and validation. J Comput Chem. 23 (2002) 1623-41.
[75] R. Islam, R. Parves, A.S. Paul, N. Uddin, S. Rahman, A. Al Mamun, N. Hossain, A. Ali, M.A. Halim, A molecular modeling approach to identify effective antiviral phytochemicals against the main protease of SARS-CoV-2, Journal of Biomolecular Structure and Dynamics. 0 (2020) 1–12.
[76] A. A. Elfik, E. B. Azzam, Novel guanosine derivatives against MERS CoV polymerase: An in silico perspective, Journal of Biomolecular Structure and Dynamics. 0 (2020) 1-12.
[77] M. Nisha, R. Sakthivel, D. Velmurugan, G.M. Michael, Computational studies of drug repurposing and synergism of lopinavir, oseltamivir and ritonavir binding with SARS-CoV-2 protease against, Journal of Biomolecular Structure and Dynamics. 0 (2020) 1-13.
[78] A. Kuzmanic, B. Zagrovic, Determination of Ensemble-Average Pairwise Root Mean- Square Deviation from Experimental B-Factors, Biophysj. 98 (2010) 861–871.
[79] M. Makosza, Phase-transfer catalysis. A general green methodology in organic synthesis, Pure and Applied Chemistry. 72 (2000) 1399–1403.
[80] K.O. Rachedi, T.-S. Ouk, R. Bahadi, A. Bouzina, S.-E. Djouad, K. Bechlem, R. Zerrouki,
T. Ben Hadda, F. Almalki, M. Berredjem, Synthesis, DFT and POM analyses of cytotoxicity activity of α-amidophosphonates derivatives: Identification of potential antiviral O,O-pharmacophore site, Journal of Molecular Structure. 1197 (2019) 196–203.
[81] S. Uzun, Z. Esen, E. Koç, N.C. Usta, M. Ceylan, Experimental and density functional theory (MEP, FMO, NLO, Fukui functions) and antibacterial activity studies on 2-amino- 4- (4-nitrophenyl) -5,6-dihydrobenzo [h] quinoline-3-carbonitrile, Journal of Molecular Structure. 1178 (2019) 450–457.
[82] M.J. Aurell, L.R. Domingo, P. Pérez, R. Contreras, A theoretical study on the regioselectivity of 1,3-dipolar cycloadditions using DFT-based reactivity indexes, Tetrahedron. 60 (2004) 11503–11509.
[83] O. V Galzitskaya, S.O. Garbuzynskiy, Radius of gyration as an indicator of protein structure compactness, Molecular Biology. (2008) 144–154.